ADDIS ABABA UNIVERSITY

SCHOOL OF GRADUATE STUDIES

Isolation and Characterization of Native Cellulose and Microcrystalline Cellulose from Teff Straw, and Evaluation of Microcrystalline Cellulose as Directly Compressible Pharmaceutical Excipient

By

Melese Getachew (B. Pharm)

Addis Ababa, Ethiopia

July, 2019

Isolation and Characterization of Native Cellulose and Microcrystalline Cellulose from Teff Straw, and Evaluation of Microcrystalline Cellulose as Directly Compressible Pharmaceutical Excipient

A Thesis Submitted to the School of Graduate Studies, Addis Ababa University in partial fulfillment of the requirements for the Degree of Master of Science in Pharmaceutics.

Melese Getachew (B. Pharm)

Advisors:

Prof. Tsige Gebre-Mariam

and

Dr. Anteneh Belete

Addis Ababa, Ethiopia

July, 2019

Addis Ababa University

School of Graduate Studies

Isolation and Characterization of Native Cellulose and Microcrystalline Cellulose from Teff Straw, and Evaluation of Microcrystalline Cellulose as Directly Compressible Pharmaceutical Excipient

By: Melese Getachew (B. Pharm)

Approved and signed by the Examining Committee:

Prof. Tsige Gebre-Mariam	_____	__/___/_____
(Advisor)	Signature	Date
Dr. Anteneh Belete	_____	__/___/_____
(Advisor)	Signature	Date
Dr. Gebremariam Birhanu	_____	__/___/_____
(Internal Examiner)	Signature	Date
Dr. Getahun Paulos	_____	__/___/_____
(External Examiner)	Signature	Date

ABSTRACT

Cellulose is one of the major components of agricultural byproducts. Teff is the most widely cultivated cereal crop in Ethiopia covering 22.95% of the cultivated land from which about 7.46 million tons of Teff straw is produced as a byproduct each year. The aim of this study was to isolate and characterize native cellulose and microcrystalline cellulose (MCC) from Teff straw, and evaluate MCC as directly compressible pharmaceutical excipient. Cellulose was isolated from Teff straw with formic/ acetic acid-based treatments and MCC was prepared through HCl catalyzed hydrolysis of cellulose. The isolated cellulose and MCC were characterized through scanning electron microscope (SEM), infrared spectroscopy (FTIR), differential thermal analysis (DTA), thermogravimetric analysis (TGA) and x-ray diffraction (XRD). Powder property, compressibility and tablet properties of MCC were also studied.

Yields of cellulose and MCC powder from the raw material were 35.2% and 27.2%, respectively. Cellulose displayed rod-shaped fibers whereas MCC showed irregularly shaped aggregated particles. The IR spectra of both cellulose and MCC, and thermogram of MCC showed similarity with that of Avicel PH-101. The degree of polymerization (DP) and crystallinity index of cellulose were 594.51 and 72.26%, respectively. Whereas, MCC powders showed DP of 241.09–257.38 and crystallinity index of 76.45–84.52%. Spray dried MCC (MCC-SD) exhibited poor flow while oven dried MCC (MCC-OD) showed passable flow property. Both MCC-SD and MCC-OD displayed lower mean particle size and wider particle size distribution than Avicel PH-101. At all compression forces studied, MCC-SD showed superior compactibility than MCC-OD. Both MCC-OD & MCC-SD showed lower lubricant sensitivity and compressibility than Avicel PH-101. Paracetamol loaded tablets of MCC-SD and Avicel PH-101 powders exhibited comparable tensile strength. Disintegration and dissolution profiles of all tablets fall within acceptable limits set for conventional tablets.

Based on the results of this study, MCC powder could be prepared from locally available alternative source (Teff straw) for pharmaceutical applications. But, critical variables of MCC preparation should be optimized in order to improve its powder and compaction properties.

Keywords: Cellulose, Microcrystalline cellulose, Oven dried Microcrystalline cellulose, Spray dried Microcrystalline cellulose, Teff straw

ACKNOWLEDGMENTS

At the very beginning, I want to express my heartfelt gratitude to the almighty God for his infinite love and blessings throughout my life.

I would like to extend my deepest gratitude and heartfelt thanks to my advisors, Prof. Tsige Grebe-Mariam and Dr. Anteneh Belete for their support, advice and mentorship during the thesis work and throughout the whole course of my postgraduate study.

I would also like to acknowledge AAU, Department of Pharmaceutics and Social Pharmacy for providing me access to laboratory facility and its staff for their cooperation and assistance; Institute of Technology, AAU for allowing me to access spray drier; Pharmacognosy Department for column chromatography study; Department of Materials Engineering, Adama Science and Technology University for DTA, TGA & XRD study; Leather industry development institute for SEM study; Ethiopian Public Health Institute for ash value determination; Ethiopian Pharmaceutical Manufacturing Sh. Co. (EPHARM) for FTIR study and supply of paracetamol powder; and East Africa Pharmaceuticals for allowing me access to tablet compression machine.

I would like to offer my special thanks to Mr. Tesfaye Gabriel for his valuable contribution to my thesis work starting from proposal development. I also want to thank Fekade Tefera, Semaw Asmare, Abite Abebaw, Abraham Wondimu and my classmates for their support during this work. Special thanks to my beloved wife Lishan Tesfaye, my parents and siblings; your support and encouragement have been vital for my success throughout my career.

Finally, I would like to thank Debre-Markos University and Addis Ababa University for sponsoring my postgraduate study and thesis, respectively.

TABLE OF CONTENTS

LIST OF FIGURES

LIST OF TABLES

ABBREVIATIONS/ ACRONYMS

AGU	D-anhydroglucopyranose units
ASTM	American Standard Test Methods
BP	British Pharmacopoeia
CF	Compression Force
CI	Compressibility index
Cuam	Cuprammonium hydroxide
DP	Degree of polymerization
DTA	Differential thermal analysis
FWHM	Full width at half maximum
FTIR	Fourier Transform Infrared Spectroscopy
HR	Hausner ratio
IR	Infrared
LSR	Lubricant sensitivity ratio
MCC	Microcrystalline Cellulose
NF	National Formulary
RH	Relative Humidity
RPM	Revolutions-per-minute
TGA	Thermogravimetric Analysis
USP	United States Pharmacopoeia
UV	Ultraviolet - Visible
XRD	X-ray Diffraction

1. INTRODUCTION

1.1. Cellulose and its Natural Sources

Cellulose is one of the most abundant substances in nature which was first isolated by the French chemist Anselme Payen in 1838 (Adler, 1977). Payen found a substance which remains resistant after treatment of various plant tissues with acids and ammonia, and after subsequent extraction with water, alcohol, and ether. He understood that the substance was not starch, but it still could be broken down into basic units of glucose just as starch does. Through elemental analysis, Payen determined the molecular formula of the substance to be $(C_6H_{10}O_5)_n$ and observed the isomerism with starch. This new substance was named "cellulose", by the French Academy in 1839, since it was obtained from the cell walls of plants (Klemm *et al.*, 2005).

The first solvent of cellulose, cuprammonium hydroxide solution (Schweizer's reagent), was prepared by Schweizer in 1857 whereas the first derivative, cellulose acetate, was synthesized by Schutzenberger in 1865 (Varshney and Naithani, 2011). Hyatt Manufacturing Company used cellulose for the first time to produce successful thermoplastic polymer in 1870, which they called celluloid, using camphor as plasticizer. This effective modification was pioneer work for an industrial scale chemical modification of cellulose. The chemical structure of cellulose was later determined in 1920 by Hermann Staudinger (Klemm *et al.*, 2005; Trache *et al*., 2016). Microcrystalline cellulose (MCC) was first prepared by Battista through hydrochloric acid catalyzed hydrolysis of cellulose (Battista, 1956).

Cellulose is the major structural polysaccharide in the cell walls of higher plants (40% to 50%), cotton (87–96%), flax (80%) and jute (60–70%) (Cui, 2005). It constitutes considerable proportion of agricultural by-products such as rice straw (30.73%) (Jiang *et al.*, 2011), wheat straw and sugarcane bagasse (40%) (Sun & Hughes, 1998). The polymer is also found in the cell walls of green algae, *Acetobacter xylinum* and related species and some fungi. It is estimated that nature produces over 7.5×10^{10} tons of cellulose each year (Trache *et al.*, 2016).

The cells in each fibre of all plant based natural fibres are formed out of crystalline microfibrils based on cellulose. These microfibrils are surrounded by a non-cellulosic matrix of lignin and

hemicellulose. Because of the presence of the three components, these sources of cellulose are usually known as lignocellulosic materials. Multiple of such cellulose-lignin/hemicellulose layers in one primary and three secondary cell walls stick together to numerous layer composites, forming the cell. The composition and orientation of these cell walls vary depending on plant sources and treatment methods employed (Bledzki and Gassan, 1999). Pectin, a collective name for hetero-polysaccharides, represents other components of lignocellulosic materials. It basically consists of poly-galacturonic acid and becomes soluble in water only after partial neutralization with alkali or ammonium hydroxide (Doesburg, 1957; Bledzki and Gassan, 1999).

In contrast to cellulose, hemicellulose is a complex, branched and heterogeneous polymeric network of pentoses (xylose and arabinose) and hexoses (glucose, galactose, mannose, rhamnose, and glucuronic and galacturonic acids). Degree of polymerization of native cellulose is usually 10–100 times higher than that of hemicellulose. Cellulose fibrils are crosslinked with the lignin matrix by hemicellulose (Bledzki and Gassan, 1999; Cui, 2005).

Lignins (Latin: *lignum* meaning 'wood'), complex hydrocarbon polymers with both aliphatic and aromatic constituents, are covalently and/ or noncovalently bound to fibrous polysaccharides within plant cell walls. Lignin holds cellulose and hemicellulose fibers together and gives support, resistance and impermeability to the plant. It is an amorphous biomacromolecule which consists phenylpropanoid units; *p*-coumaryl alcohol, coniferyl alcohol and sinapyl alcohol. The phenylpropane units are crosslinked to each other by various chemical bonds like β-*O*-4-aryl ether linkages, α-*O*-4-aryl ether, 4-*O*-5-diaryl ether, β-5-phenylcoumaran, 5-5-biphenyl, β-1-(1,2-diarylpropane) and β-β-(resinol) (Spiridon, 2018). The magnitude of cells having lignified walls often increases with plant maturity (Barros *et al.*, 2005). Next to cellulose, it is one of the most abundant organic polymers on Earth with annual production of approximately 1.1 million metric tons (Moreira *et al.*, 2013). In addition to biofuel production, lignin is reported to have diverse pharmacological activities, such as anti-tumor, antimicrobial, anti-HIV and antioxidant activities (Spiridon, 2018).

1.2. Teff Grass (*Eragrostis tef*)

Teff (*Eragrostis tef*) belongs to the family Poaceae, subfamily Eragrostoidae, tribe Eragrosteae, and genus Eragrostis with the genus containing as many as 300 species (Coleman, 2012). The word "Teff" (Amharic: ጤፍ (ṭēff); xaafii (afaan oromo)) is derived from the Ethio-Semitic root "tff": ጠፍ), which means "lost", possibly referring to its extremely small seed size (Foodcomplex.org). Teff, mainly used as grain, has been grown by Ethiopian farmers as far back as history reaches. However, the grass has been mainly cultivated as hay in other countries including Kenya, South Africa, Australia and South America. The cereal is believed to be domesticated between 4000–1000 BC (Mengesha, 1966; Roseberg *et al*., 2006).

Figure 1: Teff grass (left) (Google image) and Teff straw (right).

Teff can be cultivated under a wide range of environmental conditions such as on marginal soils under water logged to drought conditions. It can produce a crop in a relatively short growing season. It produces both grain for human food and fodder for cattle. It is a fine stemmed, annual grass with bunch appearance (Figure 1-left) which has large crowns and many tillers. The inflorescence is an open panicle and produces small seeds where 1,000 seeds

weigh about 0.3 to 0.4 g. It possesses shallow and massive fibrous rooting system. The height of teff grass varies depending upon cultivar type and growing environments (Stallknecht *et al.*, 1993).

Teff is the most widely cultivated cereal crop in Ethiopia. In the '*meher'* season (June - August) of 2015/2016, 2.87 million hectares (22.95%) of land was covered solely with Teff which was cultivated by 6.56 million farmer households (Mottaleb and Rahut, 2018). In the same year, yield of Teff grain was reported to be 1.3 tons per hectare of farm (Cochrane and Bekele, 2018). Hence, approximately 3.73 million tons of Teff grain was assumed to be produced in the country. In most cereals, approximately 2lb of straw is expected to be produced per 1lb of grain (Miller, 1975). Taking this into consideration, Ethiopia's annual production of Teff straw is estimated to reach about 7.46 million tons.

Many Ethiopian farmers use Teff straw to feed their livestock as well as construction material by mixing with mud. Despite this common practice, the use of such straws for animal feed has limitations due to their low nutritive value indicated by their high fiber (lignocellulose) contents (Abule *et al.*, 1995). Different studies reported that agricultural byproducts are known for their high level of cellulose content. For example, it is reported that wheat straw contains cellulose (43%), hemicellulose (34%) and lignin (22%) (Alemdar and Sain, 2008). Cellulose was also isolated by Nuruddin *et al.* (2011) from agricultural residues like rice straw and wheat straw with respective yields of 38.1% and 37.8%. A study conducted by Chufo *et al.* (2015) reported that Teff straw contains cellulose (36.7%), hemicellulose (32.4%) and lignin (9.4%). This study also revealed that total nitrogen comprises 1% (equivalent to 6.25% protein) of the straw. In addition, the straw contains magnesium (1.19%), calcium (3.71%) and iron (0.56%) (Wassie and Srivastava, 2016).

1.3. Methods of Cellulose Isolation from Lignocellulosic Materials

For pure cellulose to be isolated, there should be an effective method to remove hemicellulose, lignin and other impurities. Two general approaches can be followed to successfully isolate cellulose from natural sources. The first is the top-down approach, in which natural sources (wood, cotton, annual plant or other agricultural residues) are fractionated to produce a desired

quality and size of cellulose. Whereas, cellulose is biosynthesized from glucose using bacteria (e.g. Acetobacter Xylinam) in a bottom-up approach (Trache *et al.*, 2016).

Pretreatment is required to alter both the physical and chemical structure of lignocellulosic materials to make cellulose more accessible to chemicals which is an essential step for their bioconversion to desired derivatives. Various pretreatment processes, commonly categorized into physical, chemical, physicochemical, biological, and also combinations of these, have been developed for cellulose isolation (Sun *et al.*, 2016).

Hydrolytic treatment of lignocellulosics by saturated steam or hot water (autohydrolysis) has been widely studied as a method to disrupt the lignocellulosic structure. Chemical treatment with acids or bases also promotes hydrolysis and improves the quality of cellulose by facilitating removal of hemicellulose, lignin and other impurities (Wang *et al.*, 2010). Enzymes have been used in plant material processing to selectively hydrolyze several components in the plant fiber, mainly hemicelluloses and lignin, while retaining cellulosic portion (Radotić and Mićić, 2016).

In most of the methods presented above, cellulose has been isolated with the sacrifice of lignin and hemicelluloses though both of these components possess a huge potential for liquid fuel, food, feedstock, and fiber production. Hence, fractionation of biomass has been studied as an option for the simultaneous production of cellulose, lignin, and hemicellulose. In the biorefinery concept, higher value-added products such as ethanol, polymers, carbon fibers and diesel fuel are produced in addition to pulp. Physicochemical pretreatment is most commonly used to increase the reactivity of lignocellulosic structure, followed by one or more separation and purification stages to isolate products (Montané *et al.*, 1998; Van Heiningen, 2006).

Formic acid is described to be an effective, cheap and readily available chemical agent for biomass fractionation of lignocelluloses. Up on cooking of plant materials with formic acid, lignin is dissolved due to cleavage of the β-*O*-4 bonds. On the other hand, hemicellulose degrades into mono- and oligosaccharides whereas cellulose remains as solid residue (Zhang *et al.*, 2010). Lignin can be easily precipitated and separated from the black liquor by adding sufficient water. After pulping, formic acid can be recovered for reuse by distillation which

leaves residue of sugars mainly from degradation of hemicellulose. But solvent recovery is complicated because of generation of acetic acid from the bound acetyl group in hemicelluloses during formic acid-based delignification process (Jahan *et al*., 2014). Meanwhile, reactive distillation with methanol is reported to be effective in separation of formic acid and acetic acid (Painer *et al.*, 2015). Furthermore, degradation of cellulose during Formic acid/ performic acid delignification process is reported resulting in decreased yield (Mire *et al.*, 2005). Combination of formic acid and acetic acid is used to overcome this problem. Formic acid acts as proton supplier, whereas acetic acid as lignin solvent (Jahan *et al.,* 2014). Delignification rate is reported to be higher when proportion of formic acid is increased in the formic acid/ acetic acid mixture and this also resulted in decreased amounts of residual lignin (Mire *et al.*, 2005; Jahan *et al.,* 2014). Hydrogen peroxide became the preferred bleaching agent since the use of hypochlorite gives rise to subsidiary reactions leading to the formation of a number of chlorinated hydrocarbons such as the carcinogenic trichloromethane (Lacasse and Baumann, 2012).

1.4. Modification of Cellulose

The fibrous nature and large size of native cellulose make the polymer poor candidate to be used directly in different pharmaceutical applications. Flow property, density, solubility and stability are among the crucially affected parameters. In order to improve these physicochemical properties of cellulose, different derivatives have been prepared. Hydrolysis of amorphous portions with mineral acids and substitution of hydroxyl groups with different functional groups are commonly used methods of modification (Klemm *et al.*, 1998).

Cellulose ethers can be prepared by treating alkali cellulose with a number of various reagents including alkyl or aryl halides (or sulfates), alkene oxides, and unsaturated compounds activated by electron-attracting groups. Methyl cellulose and ethyl cellulose are examples of cellulose ethers which are water soluble at 1.4–2 and 0.7–1.7 degree of substitution, respectively. Another important cellulose derivative, carboxymethyl cellulose, is prepared from alkali cellulose in the presence of monochloroacetic acid. Cellulose acetate (an ester) is another important derivative which is prepared by the reaction of acetic anhydride with cellulose in the presence of sulfuric acid (Candido and Goncalves, 2016).

One of mostly implemented methods of cellulose modification is mineral acid catalyzed hydrolysis to yield highly crystalline and lower particle sized powder, microcrystalline cellulose (Battista, 1950).

1.5. Microcrystalline Cellulose

The microcrystals in natural cellulose are packed side by side tightly in the fiber direction, joined by amorphous hinges, in a compact structure resembling bundles of wooden matchsticks. The most common method of converting cellulose to useful products is a straight forward hydrolysis to yield microcrystalline cellulose (MCC). Method of acid hydrolysis of cellulose to obtain lower molecular size, DP, and higher crystallinity was first investigated by Battista in 1950 (Battista, 1950). The amorphous hinges are removed by severe hydrolysis with mineral acid, yielding cellulose at the so-called "level-off degree of polymerization", $\overline{\mathrm{DP}}$. The microcrystals are then de-aggregated from their fibrous, packed structure by mechanical shearing, commonly performed in a water slurry. The resulting form of cellulose is called microcrystalline cellulose (MCC) (Battista and Smith, 1962).

Differences in the kinetics of hydrolysis between amorphous and crystalline domains is the main reason for selective removal of amorphous portions and hence increment of degree of crystallinity. This hypothesis assumed that disordered (amorphous) domains are regularly distributed along the microfibers and therefore more susceptible to acid attack than crystalline regions. Moreover, homogeneous crystallites are supposed to be generated after acid hydrolysis (Schurz and John, 1975; Alemdar and Sain, 2008).

Typical parameters to be controlled include acid concentration, temperature, agitation speed and duration of hydrolysis. The nature of the acid and acid-to-fiber ratio are also important parameters that affect the properties of resulting MCC. Hydrochloric and sulfuric acids have been extensively used for the preparation of MCC though phosphoric and hydrobromic acids have also been reported for such purposes. The use of sulfuric acid, however, results in introduction of negatively charged sulphate groups (at reducing end groups) which impedes thermal stability of the microcrystals (Jahan *et al.*, 2011). The production of MCC is, hence, obviously a low-cost process. Microcrystalline cellulose is capable of forming architectural

patterns entirely different from any previously known cellulose structure. It has a higher degree of crystallinity because of partial degradation of the amorphous portions (Battista and Smith, 1962).

Both gymnosperms (generally conifers) and other softwoods, and hardwood dicotyledons are used for production of commercially available MCC. These sources differ considerably in chemical composition (proportions of cellulose, hemicelluloses and lignin) and structural organization. This affects the composition of the extracted α-cellulose and the composition and crystallinity of MCC finally produced. In addition to the wood pulp, purified cotton linters obtained from *Gossypium* species are also common sources of cellulose and its derivatives (Landin *et al.,* 1993b).

Powder MCC is usually made by spray-drying the aqueous suspension of hydrolyzed and de-aggregated cellulose. It is white, odorless, tasteless, neutral, nonreactive free flowing versatile excipient with DP value of less than 350 and average particle size ranging from about 10–100 μm. Its physico-chemical and rheological properties make it a filler & binder of choice in a variety of pharmaceutical preparations. It has been also used in many topical preparations due to its inert, non-irritating and nontoxic properties. It has good thermal stability over a wide range of temperature. It was first commercialized under the brand name Avicel®. FMC Corporation introduced Avicel® with different grades to the pharmaceutical industry, in 1962, as an ingredient for direct compression tableting (Klemm *et al.,* 2005; Trache *et al.,* 2016).

1.6. Physicochemical Properties of Cellulose and Microcrystalline Cellulose

The mechanical and physicochemical properties of natural fibres depend on the cellulose type because each type of cellulose has its own cell geometry (Bledzki and Gassan, 1999). The main difference between cellulose and MCC is that the later has lower molecular size, DP, but higher degree of crystallinity. As a consequence, most of the physicochemical properties discussed below are used for both cellulose and MCC.

1.6.1. Chemical Structure

The molecular structure of cellulose is responsible for its supramolecular structure and this, in turn, determines many of its chemical and physical properties. Cellulose is a linear homo-polysaccharide composed of Anhydro-D-glucopyranose units (AGUs) (Figure 2-c), which are linked together by β-1,4-glycosidic bonds (Figure 2-f). Every other unit is turned 180° with connection to the neighbor unit, forming a cellobiose unit (Figure 1.2-e) (Cui, 2005; Klemm *et al.*, 2005).

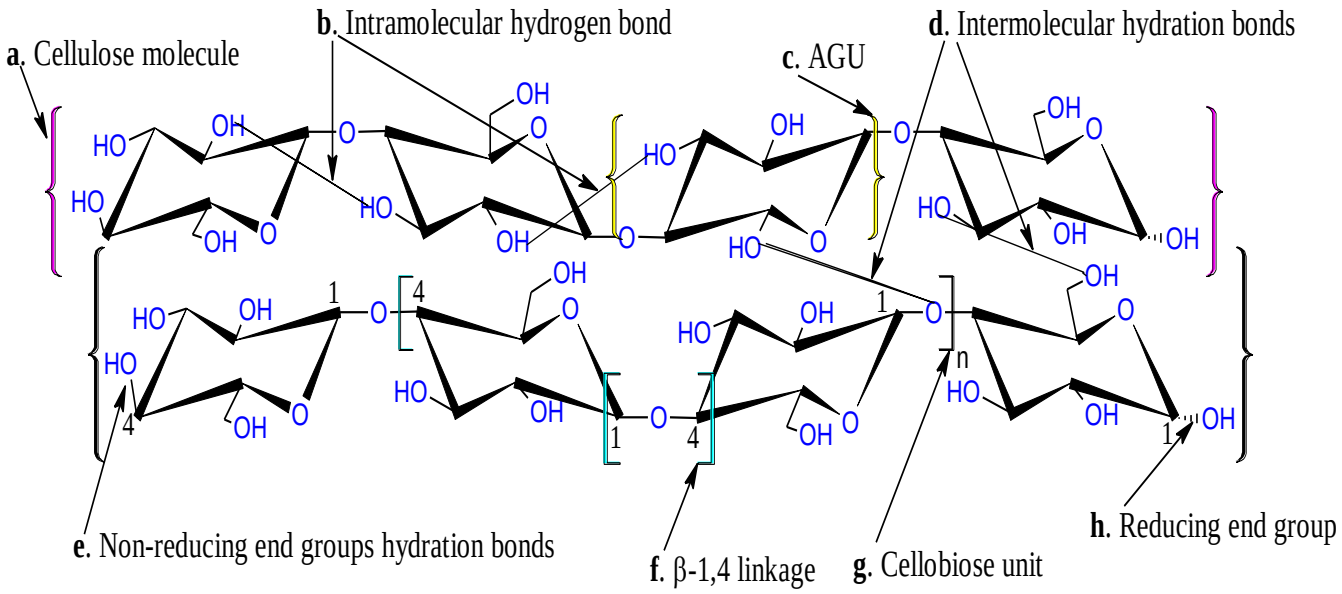

Figure 2: Chemical structure of cellulose (Cui, 2005; Habibi et al., 2010)

Additionally, cellulose molecule consists of the reducing and non-reducing end groups. The reducing end group (Figure 2-h) possesses a free hemiacetal (aldehyde) at C-1 position, whereas non-reducing end group (Figure 2-e) contains a free hydroxyl group at C-4 position. Each internal glucose unit links the neighbor unit at C-1 and C-4 positions. Furthermore, the D-glucopyranose unit has three hydroxyl groups at C-6, C-2 and C-3 positions, where the hydroxyl group at C-6 position is the most reactive, giving high functionality to cellulose. Due to the intra/inter-hydrogen bonds between these hydroxyl groups (Figure 2-b & 2-d), cellulose is insoluble in water and most common solvents. It is also resistant to the action of digestive enzymes in human small intestine but it may be fermented by colonic bacteria in large intestine resulting in production of short chain fatty acids (SCFA) (Cui, 2005; Klemm *et al.*, 2005).

Naturally, isolated cellulose molecules did not occur, assemblies of individual cellulose chain-forming fibers are found instead. This is because cellulose is synthesized as individual molecules, which undergo spinning in a hierarchical order at the site of biosynthesis. Approximately 36 individual cellulose molecules assemble into larger units known as elementary fibrils (protofibrils). The protofibrils then pack into larger units called microfibrils, which are in turn assembled into the familiar cellulose fibers. But, difference in packing of cellulose microfibrils may be encountered among different sources (Habibi *et al.*, 2010).

The chain length of cellulose, which is expressed in the number of AGUs (DP), varies with the type and nature of source and treatment methods employed. Originally, DP may range from several hundreds to thousands. While after degradation reactions, the DP value of cellulose could decrease to 300–1700. Some regenerated celluloses could even have a DP value less than 100 (Klemm *et al.*, 1998; Sun *et al.*, 2005; Jiang *et al.*, 2011). FT-IR spectroscopy is one of the most extensively used analytical tools in cellulose characterization. It is an easy and non-destructive identification method for monitoring structurally relevant information on chemical changes that occur during continuous fractionation of the polymer (Sun *et al.*, 2004).

1.6.2. Morphological Properties

The biological function and numerous applications of cellulose are dependent on its distinct fiber morphology. Elementary fibrils, microfibrils and microfibrillar bands with respective lateral dimensions of 1.5–3.5 nm, 10–30 nm and in hundreds of nm are determinants of cellulose morphology. The length of the microfibrils is on the order of several hundred nano meters. These fibrils represent the construction units of cellulose fiber cell wall architecture (Klemm *et al.*,2005).

Tablet compression is reported to be influenced by morphology of MCC which is described by the length of particles (L) and their width (D). Fibrous particles with rode shape have higher L/D ratios resulting in higher tablet strengths when compared to round-shaped particles with lower L/D ratio (Obae *et al.*, 1999). Scanning electron microscope (SEM) is among commonly used techniques to study morphology (fiber size and shape) of cellulose and MCC.

1.6.3. Crystallinity and Polymorphism

It has been known that cellulose chains are biosynthesized and self-assembled into microfibrils. These microfibrils comprise of amorphous and crystalline domains. Crystalline regions are likely to be formed due to the intramolecular (Figure 2-b) and intermolecular (Figure 2-d) hydrogen bonds formed between the free hydroxyl groups present at C-2, C-3 and C-6 positions in the cellulose macromolecules. The great interest in cellulose macromolecules emanates from their properties which originates from this crystalline orientation (Klemm *et al.*, 1998; Bledzki and Gassan, 1999).

Degree of crystallinity is an expression which shows the ratio between the mass of crystalline domains and the total mass of cellulose. Although the biosynthetic mechanism is the same in all organisms, degree of crystallinity and typical dimensions are dependent on their origin. The degree of crystallinity of cellulose and MCC, as determined by X-ray diffraction (XRD), varies from 60–80% depending on various sources of cellulose. For instance, the crystalline region content is much higher in cellulose obtained from cotton (Haafiz *et al.*,2013). On the other hand, there are much higher amounts of amorphous regions for regenerated cellulose. X-ray diffraction experiments of different native cellulose sources led to the models which indicated that native celluloses differ in number and orientation of glucose units (Klemm *et al.*, 1998).

Five major crystal polymorphs of cellulose (two of which are natural) have been identified, which are designated as I_α, I_β, II, III and IV. In nature, cellulose-I_α and I_β are the most abundant crystal forms and hence are referred to as native cellulose. Cellulose-I_α and cellulose-I_β differ with respect to their crystal packing, molecular conformation and hydrogen bonding and these may influence their physical properties. The I_α-rich specimens have been found in the cell wall of some algae and in bacterial cellulose whereas I_β-rich specimens have been found in cotton, wood, and ramie fibers. The conformation of the polysaccharide chains in both lattices is similar although the hydrogen-bonding pattern is different (Bledzki and Gassan, 1999; Saxena and Brown, 2005).

Transformation of polymorphs is also a well-studied phenomenon in the field. Accordingly, the most thermodynamically stable allomorph, cellulose-II, can be formed upon treatment of

cellulose-I with aqueous sodium hydroxide (mercerization). But, the mechanism how the parallel chain arrangement of cellulose-I undergoes transition into the antiparallel orientation of cellulose-II without an intermediate dispersion of cellulose molecules is not yet understood (Klemm *et al.*, 2005). The enhanced stability of cellulose-II emanates from presence of additional hydrogen bond per glucose residue in its structure. On the other hand, cellulose-I_α transforms into cellulose-I_β through hydrothermal treatment without losing its crystallinity. Treatment of cellulose-I and cellulose-II with liquid ammonia below -30 °C and subsequently recrystallizing the sample by evaporation of the ammonia gives crystalline cellulose-III. On the other hand, heating of cellulose-III generates cellulose-IV crystalline form (Klemm *et al.*, 1998).

1.6.4. Thermal properties

Cellulose is a stiff and rigid molecule due to the presence of intra- and inter-molecular hydrogen bonds. This phenomenon is reflected in its high viscosity in solution, high tendency to crystallize and ability to form fibrillar strands. Investigation of the thermal properties of cellulose and MCC is significant in order to determine their ability to withstand elevated processing temperatures. Thermal studies are also important to qualitatively characterize the stability, compatibility and transition phases of cellulose and MCC based on their respective thermograms (Ramiah, 1970; Alemdar and Sain, 2008).

Thermal stability and pyrolysis behavior of cellulose is commonly assessed with thermogravimetry (TG), derivative thermogravimetry (DTG), differential thermal analysis (DTA) and differential scanning calorimetry (DSC). Changes in mass are recorded as function of temperature in TGA study which indicates the undergoing chemical or physical processes upon heating a sample. In case of DTA, the difference in temperature between sample and the reference material is monitored against time or temperature.

1.7. Powder Properties of Microcrystalline Cellulose

Various grades of commercial MCC powders are manufactured by different companies. They are prepared by varying spray drying conditions in order to manipulate moisture content and

the degree of agglomeration (particle size and size distribution). These different grades of MCC differ in density (bulk and tapped), mean particle size and flow property, hence, they are suitable for various pharmaceutical applications. Powder properties of MCC are not only determinants for its functionality but at the same time they are competitive (Thoorens *et al.*, 2014). According to Obae *et al.* (1999), tablet strength increased with higher length-to-width ratio, but at the same time bulk density and flow properties of the powder are hindered. Moreover, tablet properties (such as tensile strength and disintegration time) are also highly influenced by powder properties. Properties of MCC powder like molecular weight (or DP), particle size, crystallinity, surface area, moisture content and porous structure are all influenced by the extraction methods and conditions employed and the type of cellulose (Trache *et al.*, 2016).

1.8. Pharmaceutical Applications of Microcrystalline Cellulose

Microcrystalline Cellulose is widely used in the pharmaceutical, cosmetics, food and other industries. MCC powders with different particle size and moisture content have different characteristics and applications. In the pharmaceutical industry, MCC is often used as filler, binder, suspending agent, and disintegrating agent. It is one of the most widely used filler/binders in direct tablet compression. Moreover, it is used as a diluent in tablets prepared by wet granulation as well as a filler for capsules and microspheres. It also acts as disintegrant and lubricant. MCC has been used to produce relatively free-flowing powder form of viscous (oily) active ingredients through adsorption (Rowe *et al.*, 2009).

Apart from the pharmaceutical industry, MCC has been used in food, beverage and cosmetics industries as stabilizer, anti-caking agent, fat substitute, emulsifier, gelling agent and suspending agent (Trache *et al.*, 2016). The proportion of MCC in formulations varies depending on its intended use. Generally, higher concentration of MCC (20–90%) is required when it is used as filler/binder and adsorbent while lower concentration (≤ 20%) is used in case of disintegrant and anti-adherent purposes (Rowe *et al.*, 2009).

2. SIGNIFICANCE OF THE STUDY

Plant polysaccharides (including MCC) are extensively investigated for use in the development of different dosage forms since they comply with many requirements expected of pharmaceutical excipients such as non-toxicity, stability, availability and renewability. MCC powder is among widely used excipients in pharmaceutical, food and cosmetic industries with various applications (Alemdar and Sain, 2008; Rowe *et al.,* 2009). The most common natural sources of industrial cellulose are wood pulp (90%) and cotton linter (6%) (Jahan *et al.,* 2014). However, deforestation and acceleration of greenhouse effects are nowadays becoming global concerns. Also, competition among many industries such as furniture, pulp, textile and paper become challenging to provide all sectors with the required quantities of wood and cotton at a suitable price (Trache *et al.,* 2016).

Hence, interest is increasingly growing on agricultural products and byproducts as alternative industrial cellulose sources since they possess different attributes. Appreciable amount of cellulose can be obtained from these highly renewable (non-wood) sources (Heiningen, 2006). Moreover, agricultural byproducts usually demand less energy and chemical for bleaching because of lower lignin component than wood (Trache *et al.,* 2016). Agricultural byproducts, like Teff straw, are massively produced each year in countries where their economy largely depends on agriculture. In Ethiopia, Teff is cultivated in 2.87 million hectares of land annually. From this massive farming, the country's annual production of Teff straw will reach as much as 7.46 million tons (Mottaleb and Rahut, 2018).

Though there are few pharmaceutical manufacturing companies in Ethiopia, they import literally all pharmaceutical excipients (including MCC) from abroad. This requires large amount of foreign currency which in turn can put considerable burden on the country's economic growth. Apart from the impact on foreign currency, the ordered chemicals may not be delivered timely because of problems encountered in shipment, transportation, customs procedures and other related issues. Hence, import substitution of these excipients will be economical in terms of both time and money.

To the investigator's knowledge, properties of cellulose from Teff straw have not been studied and MCC had not been prepared from Teff straw cellulose. In this study, cellulose was isolated from Teff straw and MCC was prepared by acid hydrolysis. The study tried to determine the yield and physicochemical properties of native cellulose and MCC, and the potential application of MCC as a directly compressible filler/binder.

3. OBJECTIVES OF THE STUDY

3.1. General Objective

- To isolate and characterize native cellulose and MCC from Teff straw, and evaluate MCC as directly compressible pharmaceutical excipient.

3.2. Specific Objectives

- To isolate and characterize cellulose from Teff straw;
- To prepare and characterize MCC from Teff straw Cellulose; and
- To evaluate MCC from Teff straw as directly compressible pharmaceutical excipient.

4. EXPERIMENTAL

4.1. Materials

4.1.1. Plant Material

Teff straw was collected from Enemay Woreda, East Gojjam Zone, Amhara Region.

4.1.2. Chemicals and Solvents

The chemicals used in this study were Acetic acid (99.5%) (Sigma-Aldrich, Germany), Formic Acid (85%), Cupric Sulphate Pentahydrate (98.5%), Potassium Iodide, Zinc Chloride (97%), Xylene (98%, extra pure) & Silica gel (manufactured by Loba chemie, India). Other chemicals used were Hydrogen peroxide (30%) (Carlo Erba reagents, France), Sodium Hydroxide (98%) (Alphax chemical industry, India), Hydrochloric Acid (37%) (BDH chemicals ltd, Poole, England), Ammonium Hydroxide solution (28%) (Carlo Erba reagents, France), Iodine (Hayashi pure chemical industries ltd), Sodium Chloride (99.8%) (Oxford Laboratory, Mumbai, India), MCC (Avicel® PH-101), Diethyl ether (Central Drug House Ltd, India), Magnesium stearate (Bulvinos Chemicals Ltd, England), and Paracetamol powder (China Associate Co Ltd, China).

4.2. Methods

4.2.1. Cellulose Isolation from Teff Straw

During the preliminary work, four different pretreatment methods were used for cellulose isolation. In all the methods, Teff straw was washed with tap water, air dried and ground prior to any treatment. The first isolation was conducted using alkali and steam pretreatment. Initially, the raw material (25 g) along with 500 mL of 2% NaOH was agitated at 250 rpm for 30 min and subsequently treated in autoclave at 120 ^{o}C for 60 min. The liquid part was strained through nylon cloth and the residue was washed with distilled water. It was then boiled for an hour in presence of 200 mL solution of 0.5M NaOH and 2% H_2O_2 at 60 ^{o}C. This step was repeated three times using similar amounts of fresh reagents. Following washing and filtration,

the residue was treated with 200 mL of 1M NaOH solution for 3 h; straining and addition of new alkaline solution was done after each hour. Finally, the residue was washed repeatedly with distilled water, filtered and dried at 50 ^{o}C to constant weight in oven (Kottermann® 2711, Germany) (Padmadisastra and Gond, 19989; Golbaghi *et al.*, 2017).

In hot water pretreatment, 300 mL of distilled water was added to 40 g of the straw which was then kept in water bath at 55 ^{o}C for 2 h. After straining the liquid through nylon cloth, the residue was treated with 300 mL 0.5 M NaOH for 30 min at 55 ^{o}C. Following straining, it was then bleached with 1% H_2O_2 in 200 mL 0.5 M NaOH for 1 h at 70 ^{o}C. This step was done three times and straining was done at the end of each process. The residue was then treated with 200 mL of 2M NaOH at 55 ^{o}C for 1 h. Finally, the insoluble fraction was repeatedly washed with distilled water and oven-dried to constant weight at 50 ^{o}C (Sun *et al*., 2004; Golbaghi *et al*., 2017).

In case of formic acid pretreatment, 85 mL of 85% formic acid was added to 10 g of Teff straw. It was then boiled in water bath at 92.8 ^{o}C for 2 h. After straining through nylon cloth, the residue was washed with fresh formic acid and boiled in water bath for 2 h at 80 ^{o}C along with 11.5 mL H_2O_2 and 73.5 mL of 85 % formic acid. Next, it was washed with 80% fresh formic acid. Bleaching was then done using 100 mL solution of 8% H_2O_2, 2 g NaOH and distilled water at 80 ^{o}C. Finally, it was repeatedly washed with distilled water, filtered by nylon cloth and oven-dried to constant weight at 50 ^{o}C (Jahan, *et al*., 2011).

The other batch was extracted with formic/ acetic acid pretreatment. Accordingly, isolation of cellulose was conducted with three successive treatments. Initially, it was boiled with 85% formic acid and 99.5% acetic acid (70:30) at 1:8 fibre-to-liquor ratio in water bath at 100 °C for 90 min. After straining through nylon cloth, the residue was washed with distilled water and further delignified in water bath for 90 min at 100 °C along with 10% H_2O_2, 85% formic acid and acetic acid (2:1:1 volume ratio). Following filtration and washing with distilled water, the residue was bleached with 10% H_2O_2 for 60 min in boiling alkaline medium (4% NaOH) with 1:10 fibre-to-liquor ratio. Finally, it was repeatedly washed with distilled water, strained by nylon cloth and oven-dried to constant weight at 50 °C (Mire *et al.*, 2005; Jahan *et al*., 2011; Jahan *et al*., 2014).

The cellulose characterized in this study was isolated with formic/ acetic acid pretreatment. The MCC powder characterized and compressed was also prepared following this extraction.

4.2.2. Preparation of Microcrystalline Cellulose

MCC was prepared following the method developed by Battista (Battista, 1950). A volume of 2.5N HCl was poured into volumetric flask and boiled on a hot plate. Sample of cellulose was added to the boiling acid (1:20 fibre-to-liquor ratio) and allowed to boil for 30 min at 105 °C with constant agitation (125 rpm). After completion of the reaction time, the mixture was washed, at room temperature, with distilled water followed by 5% ammonium hydroxide solution. It was then washed repeatedly with distilled water till the filtrate became clear and odorless (Battista and Smith, 1962).

The resulting MCC was dried in hot air oven (Kottermann® 2711, Germany) at 100 °C until constant weight was achieved. Finally, it was ground using glass mortar and pestle and sieved through mesh number 224 and labeled MCC-0. Other MCC powders (MCC-OD & MCC-SD) were prepared with similar conditions of hydrolysis as MCC-0 but, in this instance, the hydrolyzed cellulose was milled with juice blender for 2 min as a slurry in water. In case of MCC-OD, the material was dried in hot air oven till constant weight was achieved and then pulverized. Whereas, MCC-SD powder was prepared by spray drying of the milled slurry at 16% consistency with Tall Form Spray Drier (FT80, England) at inlet and outlet temperatures of 175 °C & 120 °C, respectively, and air pressure of 1bar (Battista and Smith, 1962, Peng *et al.,* 2012).

4.2.3. Identification Tests

4.2.3.1. Reaction with Iodinated Zinc Chloride

Initially, Iodinated zinc chloride solution was prepared by dissolving 20 g of zinc chloride and 6.5 g of potassium iodide in 10.5 mL of water. Then, 0.5 g of iodine was added and shaken for 15 min. Ten milligrams of cellulose or MCC samples were placed on a Petri dish and dispersed in 2 mL of iodinated zinc chloride solution. The resulting color of the substance was observed (BP, 2009).

4.2.3.2. Determination of Degree of Polymerization

Degree of polymerization (DP) of cellulose and MCC samples were determined with the method described elsewhere using cuprammonium hydroxide (Cuam) $[Cu(NH_3)_4(H_2O)_2](OH)_2$ solution as solvent. Cuam was prepared from freshly precipitated copper hydroxide and ammonium hydroxide solution. Initially, 28 g of $CuSO_4 \cdot 5H_2O$ was dissolved in 600 mL distilled water to which 14 mL of NH_4OH (25%) was added and the precipitate, $Cu(OH)_2$, was filtered and repeatedly washed with distilled water to make it sulfate free. The precipitate was then dissolved to 500 mL with NH_4OH (25%) to form Cuam solution. Finally, certain amount of cellulose or MCC was dissolved in the freshly prepared Cuam solution at 25 ^{o}C for about 5 min (Klemm *et al.*, 1998, Karande *et al.*, 2011).

An appropriate volume of the solution was then transferred to Ostwald viscometer. The flow times (in seconds) of blank Cuam solution (t_0) and cellulose or MCC solution (t) between the 2 marks on the viscometer were recorded and specific viscosity was determined from Eqn. 1:

$$\eta_{spec} = \left(\frac{\eta}{\eta_0} - 1\right) \quad \text{..... 1}$$

Where, η_{spec} = specific viscosity, $\frac{\eta}{\eta_0}$ = relative viscosity and η & η_0 are the time (seconds) required for the sample and blank solutions, respectively, to travel from upper to lower mark.

The DP value was then calculated from the specific viscosity according to Eqn. 2 (Klemm *et al.*, 1998; Karande *et al.*, 2011). Average value of two independent determinations was taken.

$$DP = \frac{2000\eta_{spec}}{c*(1+0.29\eta_{spec})} \quad \text{.....2}$$

Where 'c' is concentration (in g/L) of cellulose or MCC, and 0.29 is viscometer constant.

Average viscosity molecular weights of cellulose and MCC samples were determined as product of their respective DP value and the molecular weight of monomer units (162g/mole).

4.2.4. Determination of Percent Yield

The yield of cellulose and MCC from Teff straw were determined based on the dry weight basis of three simultaneous extractions. Percent yields of cellulose (Eqn. 3) and MCC (Eqn. 4) were calculated using weights of raw material and cellulose, respectively.

$$\text{Yield of cellulose (\%)} = \frac{\text{Weight of cellulose obtained (g) X 100\%}}{\text{Weight of dried Teff straw (g)}} \quad \text{..... 3}$$

$$\text{Yield of MCC (\%)} = \frac{\text{Weight of MCC obtained (g) X 100\%}}{\text{Weight of dried Cellulose used (g)}} \quad \text{..... 4}$$

4.2.5. Characterization of Cellulose and Microcrystalline Cellulose

In this study, the six properties presented below (moisture content, morphology, FTIR, DP, XRD and thermal studies) were used to characterize both cellulose and MCC. Whereas, the rest were used solely for MCC powders. Whenever appropriate, commercial MCC (Avicel PH-101) was used as standard for comparison of properties.

4.2.5.1. Determination of Moisture Content

Sample (3 g) of MCC was placed on pre-weighed Petri dish and weighed. Then the Petri dish was placed in an oven (Kottermann® 2711, Germany) and heated at 105 °C for 2 h. After removed from the oven, its weight was determined and drying was continued until constant weight was obtained by checking every 30 min. Triplicate studies were done and percentage of moisture was calculated as follows (Eqn. 5) (ASTM, 2003):

$$\text{Moisture (\%)} = \frac{\text{Mass loss on heating (g) X 100}}{\text{Weight of Sample used (g)}} \quad \text{..... 5}$$

4.2.5.2. Determination of Water-soluble Substances

The method specified in British Pharmacopoeia (2009) was used to determine percent of water-soluble substances. Accordingly, 5 g of MCC powder was added to conical flask containing 80 mL of distilled water. The mixture was shaken for 10 min and filtered with filter paper. The filtrate was then transferred to a beaker and evaporated to dryness on hot plate at 105 °C

without charring. Finally, the dried beaker was weighed and the weight of residue was recorded as the difference between the weights of empty beaker and the beaker with the residue. Triplicate studies were conducted and mean percentage values of water-soluble matter was then calculated.

4.2.5.3. Determination of Ether-soluble Substances

The column was developed using silica gel and ether (peroxide free). Five grams of MCC powder was placed in the chromatography column to which sufficient amount of ether was passed. Secondly, blank solvent (ether) was eluted through similarly developed column. Both the eluates were evaporated to dryness to constant weight. It was then allowed to cool in a desiccator and weighed. Similar procedures were done three times. The difference between the blank and sample eluate residues was taken as the amount of ether-soluble matter in the sample.

4.2.5.4. Hydration Capacity

Hydration capacity of MCC was determined using the method described by Kornblum and Stoopack (1973). Accordingly, one gram of each sample was placed in four 15 mL plastic centrifuge tubes mixed with 10 mL distilled water and then stoppered. The centrifuge tubes were vigorously shaken manually for 2 min. The mixture was then allowed to stand for 5 min and mixed by inverting three times. This step was repeated once and immediately centrifuged at 2000 g for 15 min on a centrifuge. After decanting the supernatant, the centrifuge tubes were stoppered and weighed. The hydration capacity was then calculated using Eqn. 6:

$$\text{Hydration Capacity} = \frac{w_s}{w_d} \ldots\ldots\ldots\ldots\ldots\ldots\ldots\ldots\ldots\ldots 6$$

Where, W_s and W_d are weights of centrifuge tube with sediment and dry sample, respectively.

4.2.5.5. Ash Value Determination

In order to determine ash value of MCC powder, the crucible was first cleaned and oven dried at 100 °C for 30 min. Following cooling for 30 min in a desiccator which contains silica gel, the crucible weight was determined. Three grams of MCC powder was placed on the crucible and heated till the smoking was stopped. The residue was then charred in furnace at 550 °C for

2 h. After cooling in desiccator for 45–60 min, weight of ash was determined. Ash value was calculated as weight percentage of the ratio of charred residue and MCC sample.

4.2.5.6. pH Determination

Two grams of MCC powder was shaken manually with 100 mL of distilled water for 5 min. The pH of the supernatant liquid was determined by using a pH-meter (Jenway, 3505, UK). Finally, mean value of triplicate determinations was taken.

4.2.5.7. Morphological Study

Morphological analysis of cellulose and MCC samples was done using scanning electron microscope (JEOL/MP-JSM-IT300) with gold coating. All images were taken at an accelerating voltage of 20 kV and magnifications of 200, 500 & 1000X.

4.2.5.8. Fourier Transform Infrared Spectroscopy

FTIR spectra of native cellulose, MCC and Avicel PH-101 samples were acquired at room temperature using FTIR spectrophotometer (FTIR-8400S, SHIMADZU, Japan) in transmittance mode. About 5 to 10 mg of samples were mixed with liquid paraffin in a mortar and pestle. The sample mixture was then spread on the surface of a potassium bromide (KBr) plate and the other KBr plate was placed on top of the first plate to form a thin film of the mull by compression between the two plates. The sandwiched plates were placed in the infrared spectrometer and the spectra were obtained. Each IR spectrum was collected with 20 scans and spectral resolution of 8 cm^{-1}. Scanning was performed between wave numbers 4000 and 400 cm^{-1}. Background spectrum was collected before running each sample and IR solution software was used for data treatment.

4.2.5.9. X-Ray Diffraction (XRD)

To determine the crystal structure and crystallinity, XRD patterns of cellulose and MCC samples were measured by automated powder X-ray diffractometer (XRD-7000S, SHIMADZU, Japan). Before testing, samples were dried in a dry oven at 100 °C for 30 min to remove moisture. The XRD data were generated by a diffractometer with Cu-Ka radiation (λ = 1.542° A) at 40 kV voltage and 30 mA current over 2θ angle range of 10°–40°, angle step of

0.02°, a time step of 0.4 seconds and scan speed of 3°/minute. The crystalline indices (CrI) of samples were calculated from the X-ray diffraction patterns based on the peak height method developed by Segal *et al.* (1959) (Eqn. 7).

$$CrI\ (\%) = \frac{I_{002} - I_{am}}{I_{002}} \quad \ldots\ldots 7$$

Where CrI represents relative degree of crystallinity (%), I_{002} is the maximum intensity (in arbitrary units) of the 002-lattice diffraction at a 2θ angle between 22–23 degrees and I_{am} is the intensity of diffraction of amorphous portion in the same units at 2θ around 18°. Intensities of both I_{am} and I_{002} were taken above the baseline at their respective positions.

Crystal size was estimated using the Scherrer equation (Eqn. 8)

$$L = \frac{0.94 \times \lambda}{\beta_{\frac{1}{2}} \times \cos\theta} \quad \ldots\ldots 8$$

Where, L is the crystal dimension (in nanometers) perpendicular to the diffracting planes with Miller indices of hkl, λ is the wavelength of X-ray radiation (λ = 1.542Å), Scherrer constant (K = 0.94) represents the shape factor (depends on the shape of the crystallites), $\beta_{1/2}$ is the full width at half maximum (FWHM) of the diffraction peaks, in radians, at a height half-way between background and the peak maximum, and θ is half of the (002) Bragg diffraction peak position (2θ max position) (Trache *et al.*, 2014; Agarwal *et al.*, 2017).

4.2.5.10. Thermal Properties

Thermal properties of samples were investigated by TGA and DTA on a simultaneous thermal analyzer (DTG-60H, SHIMADZU, Japan). Teff straw, cellulose, MCC and Avicel PH-101 samples with respective weights of 6.877 mg, 14.767 mg, 15.794 mg and 16.168 mg were used. Each sample was heated from room temperature to 700 °C using platinum cell at heating rate of 10 °C/min. Nitrogen gas was used as carrier gas to provide inert atmosphere at flow rate of 50 mL/min. Weight loss and change in temperature were recorded as a function of time and temperature.

4.2.5.11. Particle Size Analysis

Particle size analysis was performed using Malvern Mastersizer 2000 laser diffraction particle-size analyzer (Malvern Instruments Ltd, Worcestershire, WR14 1XZ, UK). After switching the instrument, the software (Mastersizer 2002) was run and parameters set. The parameters set were: range (0.05–900 µm, 300RF); active beam length (2.4 mm); sample unit (MS1: Small Volume Sample Dispersion Unit); polydisperse; standard-wet, Presentation (3OHD). About 500 mL distilled water was used in order to immerse the sampling port of the Hydro dispersion unit. Background reading was done with the dispersing medium (distilled water). Then, a small amount of MCC powder was dispersed in to the soaking distilled water till an obscuration (a measure of the amount of laser light lost due to the introduction of the sample within the analyzer beam) of 17-19% was achieved. The mean volume particle size distribution, mean particle size, specific surface area and percentile distribution of samples were determined with the software. Determinations were done in triplicates and average values with corresponding standard deviations were calculated.

4.2.5.12. Density and Related Properties

Bulk and tapped density of MCC powders were determined according to the method described in USP-30/NF-25–616 (2007) whereas Hausner ratio and Carr's index according to USP-30/NF-25–1174 (2007).

i. Bulk Density

Bulk densities of MCC powders were determined by the commonly described method, using measuring cylinder. Thirty grams (m) of MCC powder was gently poured into a graduated cylinder of 250 mL capacity (readable to 2 mL). The powder was carefully leveled with light tapping and the unsettled apparent volume (V_b) was read to the nearest graduated unit. Bulk density (g/mL) was calculated as the ratio of mass of sample and apparent volume. The average value of three independent determinations was finally taken.

$$\text{Bulk Density} = \frac{m}{V_b} \qquad \ldots\ldots\ldots\ldots\ldots\ldots\ldots\ldots\ldots\ldots\ldots\ldots .. \ 9$$

ii. Tapped Density

After determining bulk volume as described above, the measuring cylinder was secured in the holder of tapped densitometer (ERWEKA, Germany). Samples of MCC powders were tapped sequentially 10, 500 and 1250 times (plus 1250 times for subsequent taps, if necessary). Tapping was stopped when the change in volume doesn't exceed 2 mL. The tapped density was calculated from the weight and tapped volume (V_t) of the powder. Tapped density (g/mL) was determined as a mean of three measurements.

$$\text{Tapped Density} = \frac{\text{m}}{V_t} \quad \text{..... 10}$$

iii. Carr's Index and Hausner Ratio

Using bulk volume and tapped volume data, Carr's Index (percent compressibility) and Hausner Ratio were calculated by using the following equations:

$$\text{Carr's Index} = \frac{(\text{Bulk volume} - \text{Tapped volume}) \times 100}{\text{Bulk volume}} \quad \text{..... 11}$$

$$\text{Hausner Ratio} = \frac{\text{Bulk Volume}}{\text{Tapped Volume}} \quad \text{..... 12}$$

iv. True Density

True density was determined by liquid displacement method using xylene as immersion fluid. Xylene (25 mL) was added to a pre-weighed empty pycnometer, closed and weighed. After draining out the liquid, two grams of MCC samples were added into the empty pycnometer and sufficient xylene was added. After 10 min, the sedimented MCC was stirred with a glass stirrer to release entrapped air. Stirring was discontinued when evolution of air bubbles through the supernatant xylene layer had stopped. The sample was then allowed to settle and the volume was adjusted with xylene to 25 mL. True density (g/mL) was finally calculated with Eqn. 13.

$$\text{True density} = \frac{\text{W1} * \text{SG}}{[(\text{W1} + \text{W2}) - \text{W3}]} \quad \text{..... 13}$$

Where, W_1 = weight (g) of sample, W_2 = weight (g) of the pycnometer filled with xylene, W_3 = weight (g) of pycnometer with sample plus xylene, and SG = specific gravity of xylene (g/mL) which is determined from weights of empty pycnometer and pycnometer filled with xylene.

v. Porosity

The porosity of MCC powders was determined from bulk and true density using the equation described below (Eqn. 14) (Kothari, *et al.*, 2002).

$$\varepsilon = \left[1 - \left(\frac{\rho bulk}{\rho true}\right)\right] * 100 \qquad 14$$

4.2.5.13. Determination of Moisture Sorption Pattern

Five different relative humidity levels were prepared in Pyrex desiccators using distilled water (100% RH), saturated solution of NaCl (75.6% RH) and 40%, 31.58% and 24.66% of NaOH solutions (20%, 40% and 60% RH, respectively). MCC samples were pre-dried in an oven (Kottermann® 2711, Germany) for 4 h at 120 °C. Three pre-weighed dry plastic plates, each containing two grams of pre-dried MCC sample, were placed in the five different RH chambers. Samples were equilibrated for four weeks at room temperature. After four weeks, their weights were recorded and the moisture uptake of each sample was calculated as the weight difference of the MCC powder before and after equilibration in a given RH chamber. Water sorption capacities of MCC samples from each desiccator were expressed as mean percent moisture uptake of the three samples.

4.2.5.14. Drug-Excipient Interaction Study

Possible drug-excipient interaction was investigated by using FTIR spectroscopy. The FTIR spectra of paracetamol powder alone and its physical mixture with the prepared MCC powder (1:1) were recorded at 400-4000 cm^{-1} using FTIR-8400S, Shimadzu, Japan. All the procedures and parameters were similar as described in Section 4.2.5.8.

4.2.6. Preparation and Evaluation of Tablets

4.2.6.1. Tablet Compression

Tablets containing plain MCC powder were prepared to study compaction property by compressing at targeted crushing strengths of 50, 75, 100, 125 and 150 N (adjusted using Avicel PH-101) and 11mm diameter with rotary tablet machine (EC0 Press, 7891, India). Before each compression, separately weighed MCC powder (400 mg) was hand-filled to the die.

To study dilution potential, MCC powders were compressed along with different concentrations (30, 45, 60 and 75%) of paracetamol (Kuentz and Leuenberger, 2000) at a fixed compression pressure which is adjusted to give Paracetamol/Avicel (3:7) tablets with diametrical crushing strength of 80 N. Paracetamol and MCC powders were thoroughly mixed for 10 min in a Turbula® mixer (Willy A. Bachofen AG, Turbula® 2TF, Basel, Switzerland) at 45 rpm. Tablet property studies (enlisted from 4.2.6.3–4.2.6.7) were conducted for both plain MCC (prepared at CF1-CF5) and paracetamol (30-45%) containing tablets.

Tablets weighing 400 mg and containing either plain MCC powder or MCC with magnesium stearate (0.5%) were also prepared at a fixed compression pressure to study lubricant sensitivity of the filler/binders. The compaction pressure was adjusted to produce 400 mg tablets with hardness of 95 N from Avicel PH-101 and Magnesium stearate (0.5%).

Tablet properties listed from 4.2.6.3 to 4.2.6.7 were determined for MCC tablets prepared at all compression forces and all levels of paracetamol content.

4.2.6.2. Lubricant Sensitivity Ratio

The reduction in crushing strength, defined as lubricant sensitivity ratio (LSR), was used as a quantitative measure to express the sensitivity of MCC powders upon mixing with a lubricant. The LSR is the ratio between the decrease in breaking force values of tablets, due to mixing with a lubricant, and the breaking force values of unlubricated tablets.

$$LSR = \frac{BF_U - BF_l}{BF_U} \quad \text{..... 15}$$

Where BF_u and BF_l are the breaking force values of tablets prepared without and with a lubricant, respectively (Gerard and Hans, 2011).

4.2.6.3. Weight, Thickness and Diameter of Tablets

Twenty tablets were randomly selected from each batch and weighed individually on an analytical balance. The average weight, standard deviation and coefficient of variation were then calculated. Tablet thickness and diameter were measured using sliding caliper scale (Nippon Sokutei, Japan).

4.2.6.4. Crushing Strength

The diametrical crushing strength of tablets was determined with an electronic hardness tester (Caleva Model THT2, England). Values were taken as mean of ten independent determinations.

4.2.6.5. Tensile strength

The data obtained from crushing strength, diameter and thickness of tablets were used to calculate radial tensile strength using equation 16.

$$Ts = \frac{2F}{\pi DT} \quad \text{..... 16}$$

Where, Ts - the tensile strength, F - crushing strength, D - the diameter of the tablet and T - the tablet thickness.

4.2.6.6. Friability

Ten intact tablets of known weights from each batch were placed in a friability tester (ERWEKA, TAR 20, Germany) and subjected to combined effects of abrasion and shock by placing them in the plastic chamber. After challenged for 4 min at 25 rpm, the tablets were dedusted and weighed. The percent loss in weight was calculated as friability.

4.2.6.7. Disintegration Time

Disintegration test was carried out using the method stated in USP-30/NF-25–701 (2007). Six pre-weighed tablets from each batch were placed in a disintegration tester (ERWEKA, Germany) filled with distilled water at 37 ± 2 °C. The tablets were considered completely disintegrated when all the particles passed through the wire mesh.

4.2.6.8. Construction of Calibration Curve

A stock solution containing 200 µg/ml of paracetamol was prepared using phosphate buffer (pH of 5.8) as dissolution medium. From this stock solution, seven different concentrations (5.5, 7, 8.5, 10, 11.5, 13 and 14.5 µg/ml) were prepared and their UV absorbances were measured at 243 nm with UV/Visible spectrophotometer (UV Spectrometer, T92+) using phosphate buffer (pH 5.8) as a blank (USP-30/NF-25 (2007). The absorbance versus concentration of the solutions was plotted, and a linear regression equation and correlation coefficient were obtained.

4.2.6.9. *In-Vitro* Drug Release Study

Dissolution test was conducted according to the USP specification (USP30-NF25) using dissolution apparatus Type II (Paddle Method) (ERWEKA, DT600, Germany). Phosphate buffer (pH 5.8, 900 ml) was used as the dissolution medium at 37 ± 0.5 °C and stirring rate of 50 rpm. Five milliliters of aliquots of the dissolution medium were removed at 5, 10, 15, 20, 30, 45 and 60 min and filtered using filter paper. At each sampling point, equal amount of fresh medium kept at similar temperature was transferred into the dissolution vessel to keep the sink condition. One milliliter of the filtered sample was diluted to 25 mL with fresh dissolution medium and absorbance was read with UV/Visible spectrophotometer (UV Spectrometer, T92+) at 243 nm. Phosphate buffer (pH = 5.8) was used as a blank. Drug content and cumulative drug released were calculated from the absorbance data after all the necessary corrections for dilution were taken.

4.2.7. Statistical Analysis

Statistical analysis was performed using one-way Analysis of Variance (ANOVA) with statistical software Origin 7 (Origin Lab® Corporation, USA). Tukey multiple comparison test was used to compare the individual difference in physicochemical properties of MCC powders and their tablet properties. Powder and tablet properties were analyzed at 95% confidence level ($\alpha = 0.05$), hence, P-values less than 0.05 were considered statistically significant. The results are reported as mean and standard deviation (SD) of sufficient number of measurements (specified in each task). Different figures were drawn using Origin® 7 software.

5. RESULTS AND DISCUSSION

5.1. Isolated Cellulose and MCC

The various extraction methods used during preliminary study resulted in different yields and color of cellulose fibers (Figure 3-top) and MCC powder (Figure 3-bottom). The percentage yield of cellulose was 33.92 (± 2.84) (alkali and steam), 35.07 (± 1.90) (hot water), 33.85 (± 0.78) (formic acid) and 35.2 (± 2.3) (formic/ acetic acid). Though both formic acid and formic/ acetic acid pretreatments gave white cellulose fiber, the former method decreased the yield slightly (by 1.35%). This discrepancy could result from higher degradation of cellulose in the formic acid pretreatment. It is reported that increased degradation of cellulose is the common problem when formic acid is used alone for delignification. This problem worsens especially at higher acid concentration and longer duration of treatment (Jahan *et al*., 2014).

Consequently, combination of formic acid and acetic acid could help to isolate cellulose with higher yield and increased quality. The proportion of formic acid needs to be increased in the formic acid/ acetic acid mixture for efficient and fast delignification of lignocellulosic materials. Mire *et al*. (2005) reported that higher formic acid concentration sped up delignification of the vegetable matter, resulting in decreased amounts of residual lignin, and the pentosan hydrolysis. They reported that maximum delignification was achieved within 3 h when higher proportion of formic acid was used. But residual lignin content increased beyond this time of treatment which is attributed to the low solubility of lignin in formic acid and its associated precipitation on to the cellulose fiber. This solvent extraction system also ensures complete fractionation of lignocellulosics which allows recovery of the three major components; cellulose as insoluble residue, lignin as precipitate upon addition of water to spent liquor, whereas sugars after evaporation of the liquor (Mire *et al.*, 2005; Vanderghem *et al.*, 2012).

The yield of cellulose following treatment of Teff straw with formic/ acetic acid-based treatment was in agreement with a previously conducted study which reported the yield of cellulose isolated from Teff straw to be 36.7% (± 3.2) (Chufo *et al.*, 2015). The slightly decreased yield of cellulose in our study might be associated with the chemicals used,

temperature and treatment duration applied in the isolation process. In addition to formic acid, peracids are likely to be involved in cellulose degradation. Though peracids react mainly with compounds which possess aromatic groups and double bonds, the reducing end groups of cellulose could become susceptible at elevated peracid concentration and prolonged duration of exposure (Lachenal and Chirat, 2005).

Figure 3: Cellulose (top) and MCC (bottom) isolated from Teff straw following alkali & steam, hot water, formic acid, and formic/acetic acid (left to right) treatment.

Milling of the hydrolyzed cellulose was found to be important in de-aggregating the microcrystals. Its impact was reflected by differences in yield and appearance between MCC-0 and MCC-OD. Milling also facilitates the size reduction after drying of hydrocellulose. The yield of MCC-0 (fluffy powder) was only 57.5% (± 1.2) since some part of the dried hydrolyzed cellulose remained as fibrous material, even after grinding, on the surface of the sieve (No–224). Whereas, the yield of MCC-OD was found to be 77.4% (± 1.1) and 27.2%

from isolated cellulose and raw material, respectively. Yield of MCC-SD prepared from cellulose was found to be 74%. Bulk and tapped density and hence flow property of MCC powders are also improved with milling (Section 5.2.6).

5.2. Physicochemical Properties

Following formic/ acetic acid treatment, both the isolated cellulose fiber (Figure 3-top) and the prepared MCC powder (Figure 3-bottom) had white color which is in accordance with specifications. Moreover, the MCC powder have no odor and taste. In addition, both cellulose and MCC samples gave violet-blue color in iodinated zinc chloride solution. All samples of cellulose and MCC powders were completely soluble in cuprammonium hydroxide solvent (Battista *et al.,* 1956).

Table 1: Some physicochemical properties of MCC powders (OD = oven dried, SD = spray dried).

Property	Product			
	MCC-0	**MCC-OD**	**MCC-SD**	**Avicel PH-101**
DP	257.37 ± 2.40	241.09 ± 4.30	248.14 ± 4.80	226.96 ± 2.79
Mol. W_t (g/mole)	41951.56	39056.88	40199	36766.84
Water soluble substances (%) [≤ 0.25%]*	0.23 ± 0.02	0.23 ± 0.01	0.22 ± 0.03	0.19 ± 0.02
Ether Soluble substances (%) [≤ 0.05%]*	0.049 ± 0.001	0.048 ± 0.004	0.049 ± 0.002	0.022 ± 0.003
Moisture content (%) [≤ 7%]*	4.79 ± 0.9	3.1 ± 0.05	4.89 ± 0.11	5.0 ± 0.07
Hydration Capacity	2.36 ± 0.03	2.03 ± 0.005	1.95 ± 0.01	2.12 ± 0.004
p^H [5–7.5%]*	6.48 ± 0.08	6.09 ± 0.06	6.14 ± 0.04	6.27 ± 0.03
Total ash (%) [≤ 0.1%]*	0.08	0.08	0.08	0.06

* The values in parenthesis indicate Pharmacopoeial accepted values.

Both MCC-OD and MCC-SD had significantly higher ether-soluble fraction than Avicel PH-101. Percentage of water-soluble fraction, moisture content, pH and ash value of prepared

MCC powders meet the acceptable limits stated in different pharmacopoeias (Table 1). The isolated cellulose had moisture content of 6%.

The isolated cellulose had DP of 594.51 (± 3.68) and molecular weight of about 96315.5 g/mole. Different studies reported that pulps prepared following various pretreatment methods have viscosity average DP values in the range from 600 to 1000 and molecular weight 90,000 to 150,000 (Kraemer, 1938; Klemm *et al.*, 1998). These values vary largely depending not only on the sources of cellulose but also on the isolation conditions implemented. It is indicated that pulping conditions like type and concentration of chemicals used, temperature, and duration of treatment are all determinants for final DP of isolated cellulose. According to Sun *et al*. (2004), cellulose with mean DP value of 991.2 and 822.5 were isolated following 20 min treatment of delignified fiber with acetic acid (80%)/ nitric acid (70%) mixture (10:1) at 110 °C and 120 °C, respectively.

Another study stated that continuous depolymerization of cellulose is encountered as the severity of pretreatment increases resulting in low molecular weight polymers. By varying the pretreatment conditions, cellulose isolated from wheat straw and rice straw exhibited respective DP values of 532–1659.2 (varying temperature and time) (Sun *et al.*, 2005) and 357–1078 (varying steam pressure and time) (Jiang *et al.*, 2011). Bleached rice hull and bean hull, pretreated with different acids, are also found to possess low DP values (Adel *et al.*, 2011). They reported that HCl pretreated bleached rice and bean hulls had respective DP of 565 and 568 while their respective DP values following H_2SO_4 treatment were 407 and 336.

Following acid hydrolysis of cellulose isolated from different natural sources, leveling of degree of polymerization of cellulose was reported to be in the range 140–350 (Battista, 1956). A statistically significant reduction of DP ($P < 0.01$) was encountered with hydrolysis of the isolated cellulose. The DP value of all the prepared MCCs and Avicel PH-101 powders are consistent with this commonly reported value. All prepared MCC powders showed significantly higher DP value than Avicel PH-101 ($P < 0.05$). Though not statistically significant, DP of MCC-OD was lower than MCC-SD which might be associated with the pulverization employed after drying in the former product.

5.2.1. Morphological Study

SEM images of cellulose and MCC-SD obtained at different magnification are presented in Figure 4 (left and right, respectively). As seen below, the isolated cellulose displayed distinct elongated rod-shaped fibers. The surface of cellulose fibers has flattened appearance. Whereas, MCC-SD powder exhibited irregular-shaped morphology in its aggregates. There are also few well-defined MCC particles with rod shape.

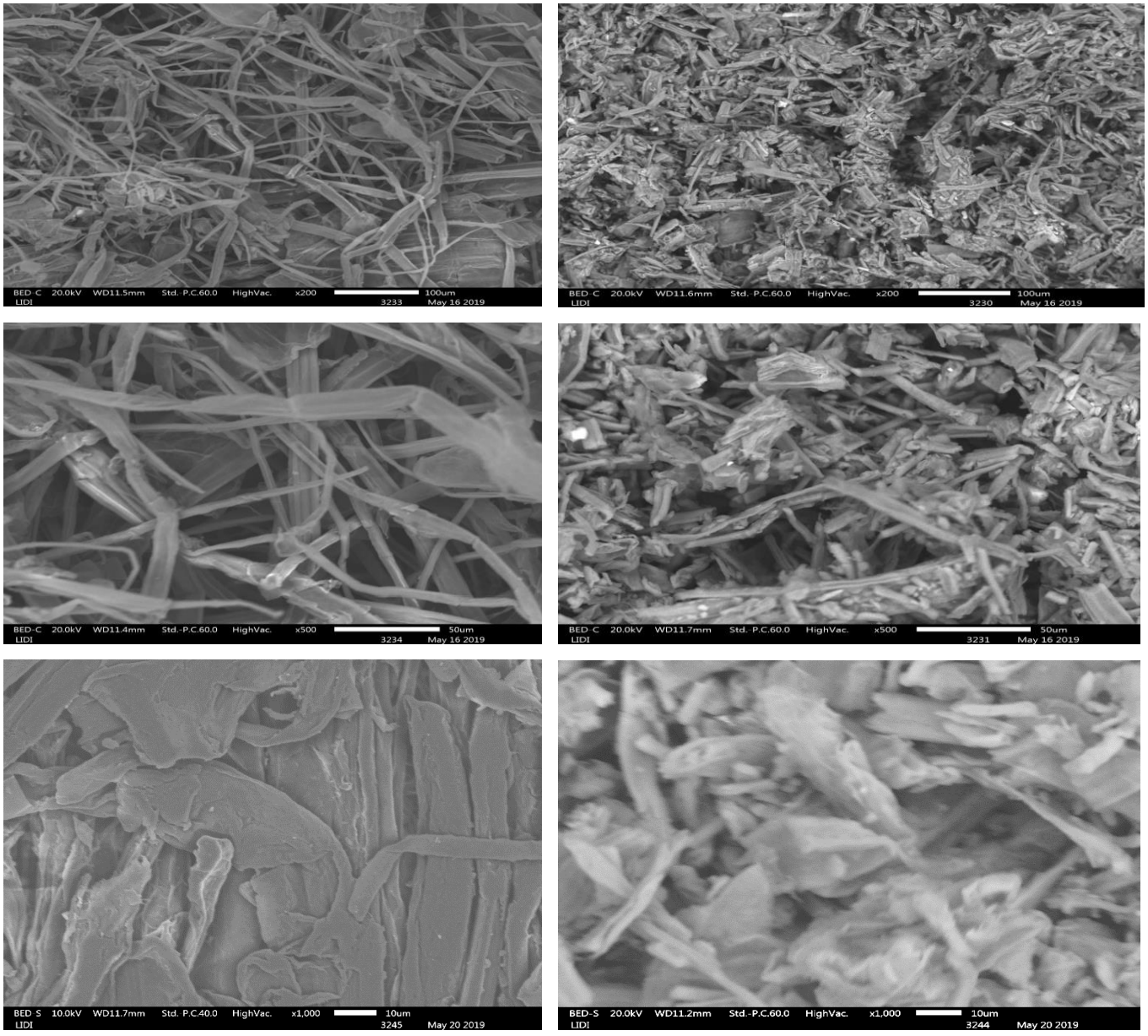

Figure 4: SEM micrographs of cellulose (left) and MCC-SD (right) with magnifications of 200x (top), 500x (middle) & 1000x (bottom).

5.2.2. FTIR Study

Two regions of IR-spectrum, lower (500–1700 cm^{-1}) and higher (2800–3500 cm^{-1}), are generally considered important for characterization of cellulose (Haafiz *et al.*, 2013). The IR spectra of Teff straw cellulose, MCC and Avicel PH-101 (recorded in the region of 4000–400 cm^{-1}) are illustrated in Figure 5, 6 & 7, respectively. With the exception of absorbed water in case of cellulose, similarities between the three spectra were observed which is an indication that the samples have similar chemical compositions. The absorption band at 1635 cm^{-1} in cellulose spectrum (Figure 3.3) might be observed due to the bending mode of the absorbed water (Sun *et al.*, 2005). Compared with both MCC and Avicel PH-101, cellulose spectrum displayed higher intensity (lower percent transmittance) at the important peaks discussed below. This could probably be encountered because of increased intermolecular interactions owing to its higher DP value compared with both the prepared and commercial MCC powders. But this should be carefully interpreted because increased amount (higher concentration) of sample will also contribute for increased IR intensity (Stuart, 2004; Silverstein *et al*., 2011).

Characteristic C=C aromatic skeletal vibrations found in lignin are usually represented by presence of two peaks in the region 1509–1609 cm^{-1} and around 1433 cm^{-1}. Since characteristic bands of lignin are absent in the cellulose spectrum, it is possible to argue that the polymer is effectively removed by chemical treatments applied. The purity of isolated cellulose is further confirmed by absence of peaks around 1730 cm^{-1} which is attributed to either the acetyl and uronic ester groups of the hemicelluloses or the ester linkage of carboxylic group of the ferulic and p-coumeric acids of lignin and/or hemicelluloses (Sun *et al*., 2005; Haafiz *et al*., 2013).

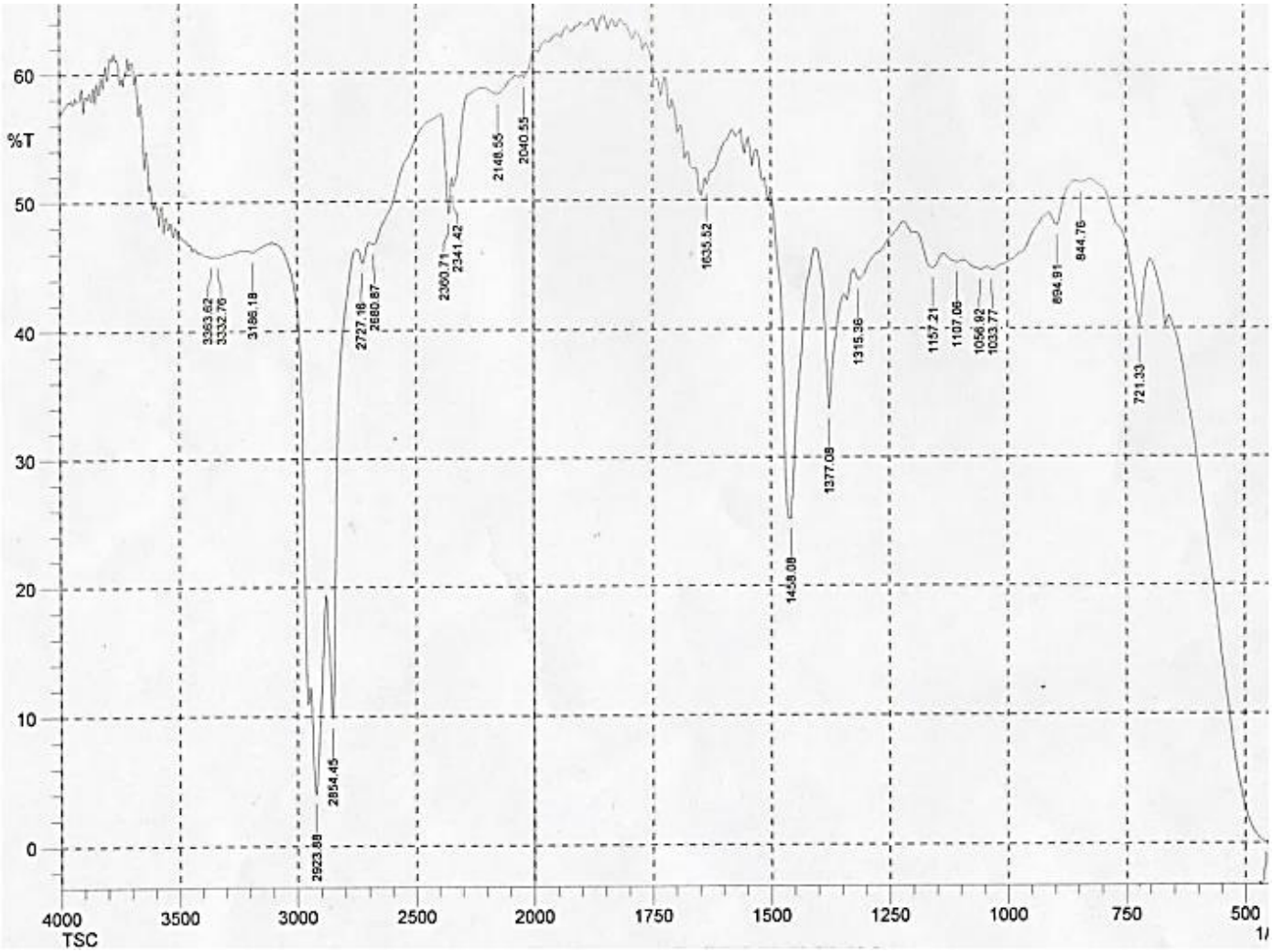

Figure 5: Infrared spectrum of cellulose isolated from Teff straw.

The absorbances at 1377 cm^{-1}, 1315 cm^{-1} (Avicel PH-101 at 1313 cm^{-1}), 1157 cm^{-1} (Avicel PH-101 at 1161 cm^{-1}), 1057 cm^{-1} (Avicel PH-101 at 1055 cm^{-1}) and 895 cm^{-1} are associated with the typical values of cellulose spectrum (Sun *et al.*, 2005). Strong peaks of O-H stretching vibrations are reflected with broad band in IR-spectra of all samples in the region 3150–3400 cm^{-1}. The absorption bands in the region around 2852 cm^{-1} and 2923 cm^{-1} originate from symmetric and asymmetric C-H_2 stretching vibrations, respectively (Stuart, 2004). In all samples, C-H_2 symmetric deformations are reflected by a sharp peak at 1458 cm^{-1} (Adel *et al.*, 2010), whereas asymmetric deformations are seen at 1377 cm^{-1} (Sun *et al.*, 2005). The band at

1313 cm^{-1} (1315 cm^{-1} for Avicel PH-101) is associated with CH_2 rocking vibration at C-6 position (Fan *et al.*, 2012).

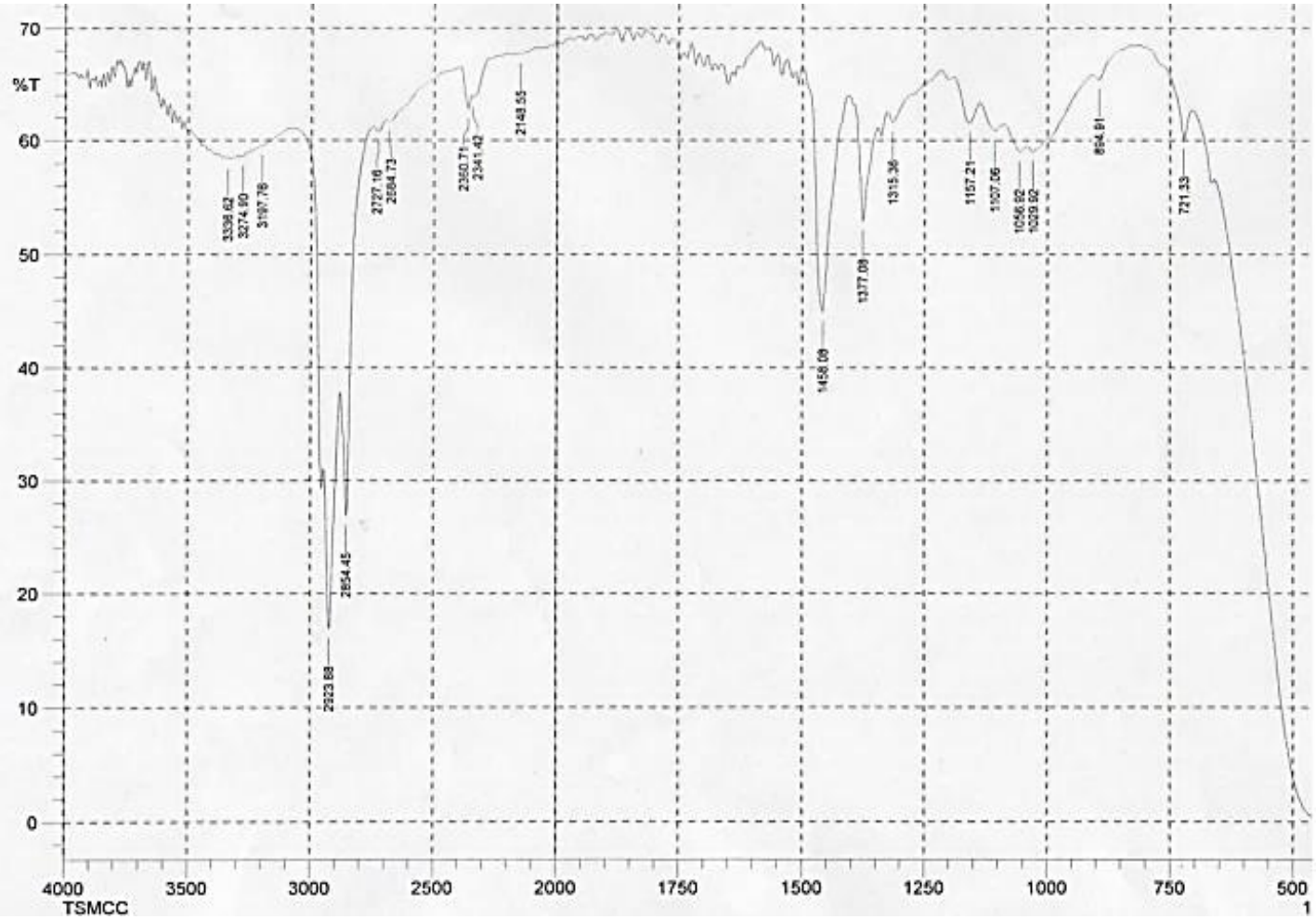

Figure 6: Infrared spectrum of MCC prepared from Teff straw cellulose.

The absorption band at 1157 cm^{-1}, in case of the two samples (1161 cm^{-1} for Avicel PH-101), corresponds to C-O-C asymmetrical stretching of β-1,4-glycosidic linkage (Trache *et al.*, 2016). The band at 1057 cm^{-1} in case of cellulose and MCC, and at 1055 cm^{-1} for Avicel PH-101 are observed due to C-O stretching vibrations (Alemdar and Sain, 2008). Rocking vibrations due to C-H bonds (anomeric vibration), which are specific for β-glucoside linkages between glucose units in cellulose, are also observed with weak band at 895 cm^{-1} in all the samples (Marchessault, 1962; Trache *et al.*, 2016).

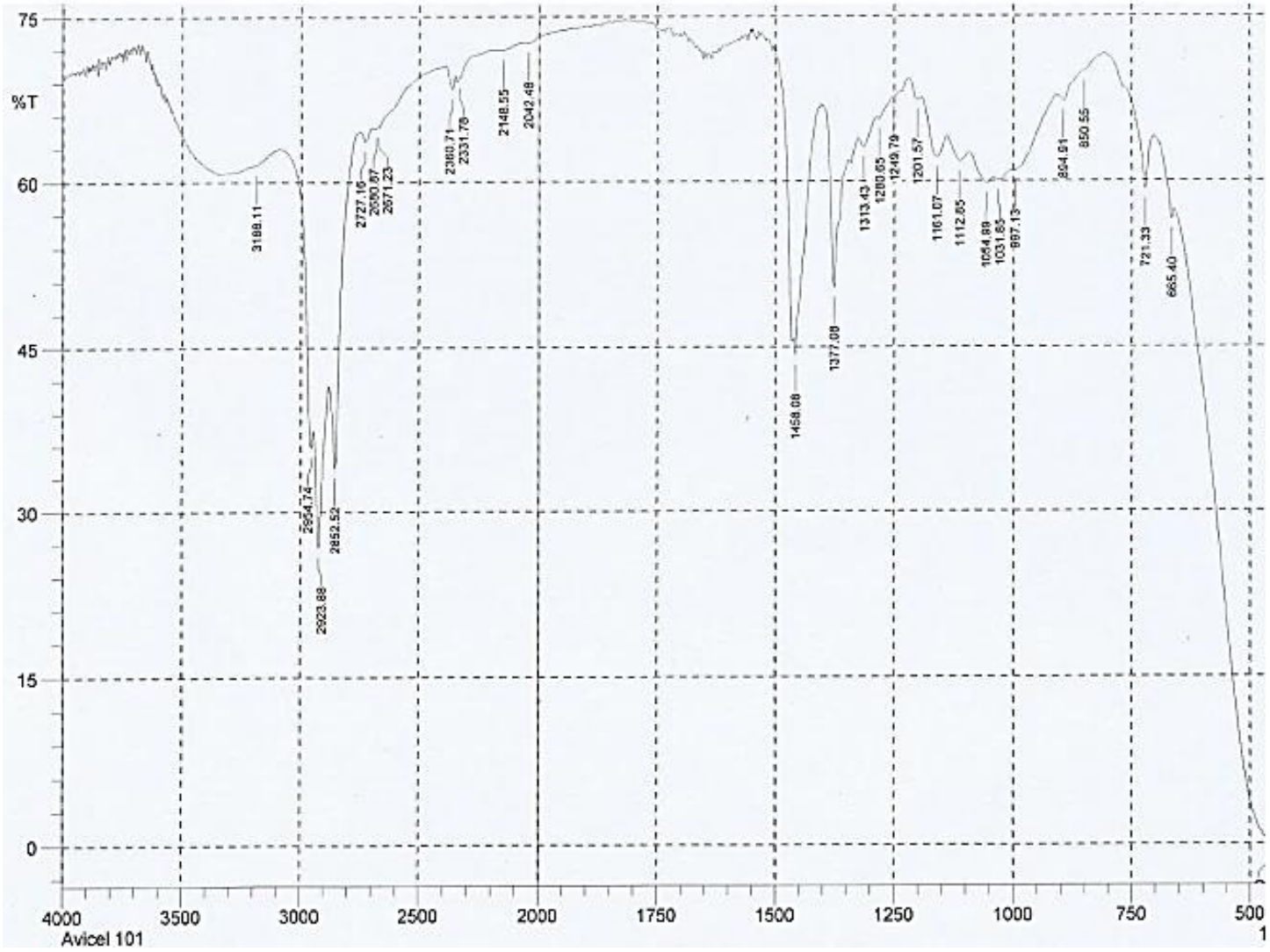

Figure 7: Infrared spectrum of Avicel PH-101.

5.2.3. X-Ray Diffraction Analysis

X-ray diffraction (XRD) gives information directly related to the crystal and amorphous portions of cellulose. Crystalline cellulose gives strong signals with sharp peaks while amorphous (non-crystalline) portion is represented by weak and broader signals in the diffraction pattern (Karimi and Taherzadeh, 2016). As clearly seen from the diffractograms (Figure 8), there is no doublet peak at the 002 plane which indicates that all the samples are comprised of cellulose-I polymorph without cellulose-II (Haafiz *et al.*, 2013). This is also supported by the IR spectrum of cellulose (Figure 5) and MCC (Figure 6) where absorbance

at 1315 cm^{-1} is seen which corresponds with CH_2 wagging of cellulose-I (Klemm *et al.*, 1998). The peak positions and intensities of both amorphous and crystalline regions along with crystallinity index and crystal size of all samples are presented in Table 2.

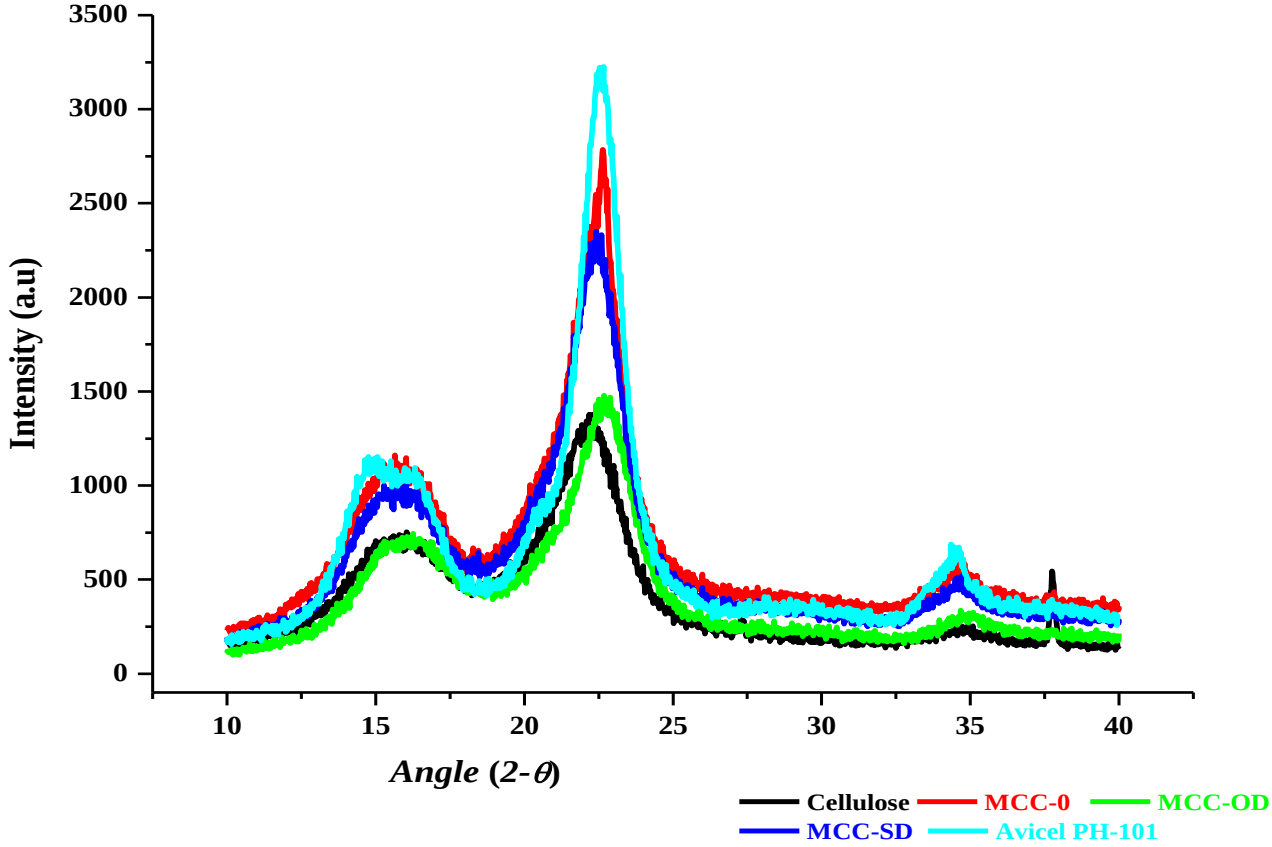

Figure 8: X-ray diffraction patterns of cellulose and various MCC powders (OD = oven dried, SD = spray dried).

The isolated cellulose and the prepared MCC powders showed closely related XRD patterns with Avicel PH-101 (Figure 8). The amorphous (I_{am}) and maximum intensity (I_{002}) peak positions were located in the angle (*2-θ*) range of 18.04°–18.94° and 22.30°–22.68°, respectively. Differences in peak height and width are observed between the samples which are expected to have encountered due to differences in their degree of crystallinity and crystal size (Wang *et al.*, 2010). Degree of crystallinity was increased by 12% through HCl catalyzed hydrolysis of cellulose. The highest crystallinity index value of MCC-0 likely has resulted due to removal of the amorphous regions of cellulose by acid hydrolytic cleavage of 1,4-glycosidic

bonds (Battista, 1950). With the hydrolysis conducted, crystal size was also increased from 2.64 nm (cellulose) to 3.82 nm (MCC-0). Among MCC powders, MCC-OD showed the shortest peak height (lowest degree of crystallinity) whereas intensity of Avicel PH-101 displayed the longest peak (highest degree of crystallinity) (Figure 8; Table 2). Different previous studies also reported consistent crystallinity index values of Avicel PH-101 with the result found in this study; 92.97% (Dourado *et al.,* 1998), 91.7% (Park *et al.,* 2009) and 88% (Terinte *et al.,* 2011).

Table 2: Crystalline properties of cellulose and MCC powders (OD = oven dried, SD = spray dried).

Parameter		Product				
		Cellulose	**MCC-0**	**MCC-OD**	**MCC-SD**	**Avicel PH-101**
Peak position (*2-θ*)	$\mathbf{I_{002}}$	22.30	22.64	22.68	22.42	22.66
	$\mathbf{I_{am}}$	18.24	18.04	18.94	18.16	18.74
Intensity (a.u)	$\mathbf{I_{002}}$	1378	2786	1480	2352	3226
	$\mathbf{I_{am}}$	414	539	394	502	412
$\beta_{1/2}$ (°)		2.57	2.57	2.99	2.58	1.77
CrI (%)		**72.26**	**84.52**	**76.45**	**82.19**	**89.9**
L (nm)		**2.64**	**3.82**	**2.83**	**3.28**	**4.78**

Degree of crystallinity of MCC is mostly reported in the literature to be in the range from 60% to 80%. But, different authors reported that highly crystalline MCC powders could be prepared from natural sources. MCC prepared from oil palm empty fruit bunch was shown to have degree of crystallinity of 87% (Haafiz *et al.,* 2013). Adel *et al*. (2011) also showed that MCC powders with degree of crystallinity of 87–92% were prepared with HCl and H_2SO_4 catalyzed hydrolysis of bean and rice hulls.

Among the prepared MCC powders, MCC-0 had the highest apparent degree of crystallinity (84.52%), whereas the lowest value was recorded by MCC-OD (76.45%). Though source of cellulose is recognized as the main determinant for crystallinity of MCC powder (Landín *et al.*, 1993a), method of manufacturing also plays pivotal role (Doelker *et al.,* 1987). Nelson and O'Connor (1964) reported that an apparently completely amorphous cellulose can be produced

by extensive milling. Since milling of the hydrolyzed cellulose was done in case of both MCC-OD and MCC-SD, it is not surprising to have lower degree of crystallinity compared with MCC-0. Similarly, the lower degree of crystallinity of MCC-OD, compared to MCC-SD, could be due to the pulverization process conducted after drying in the former product. As indicated by another study, degree of crystallinity of MCC powders was reduced from 65% to 12.1% through grinding in a vibratory mill (which involves friction as main mechanism) for 30 min (Suzuki and Nakagami, 1999).

The low crystallinity index value of MCC-OD could also be associated with its low moisture content (Table 1). The impact of moisture content should not be underestimated since the amorphous portions may become more ordered (crystalline) in hydrated state which results in different crystalline property (Park *et al.*, 2009; Agarwal *et al.*, 2017). Agarwal *et al.* (2017) indicated that crystal properties of Avicel PH-101 vary depending on whether the material is found in dry or hydrated state. According to this study, dry and moist (5%) Avicel PH-101 had respective crystallinity index values of 88.4% and 96.3%, FWHM of 1.87° and 1.56° and crystal size of 4.3 nm and 5.2 nm (Agarwal *et al.,* 2017). Park *et al.* (2009) also reported that a 5% increment of crystallinity index was found up on hydration of cellulose.

Among the MCC samples, the highest estimated average crystal size value (smallest peak width) was displayed by Avicel PH-101 (Table 2). Whereas, MCC-OD had lowest crystal size and highest peak width which might be associated with lowest degree of crystallinity (Trache *et al.*, 2014). The higher crystallite size value of MCC-0, compared with both MCC-SD and MCC-OD, could also show the narrow pattern of crystallite size distribution (Lu and Hsieh, 2012).

5.2.4. Thermal Properties

Investigation of thermal properties of cellulosic products is important to determine their stability in processing temperatures and for qualitative studies. Thermograms (TGA and DTA) of Teff straw, cellulose, MCC-SD and Avicel PH-101 are presented below (Figure 9 & 10). As clearly seen from the thermograms, thermal properties of the samples displayed three major weight loss stages with different rate and extent. The main processes involved in cellulose

degradation are identified to be dehydration, decarboxylation, depolymerization and decomposition of glycosyl units (Trache *et al.*, 2014).

On heating up to 325 °C, MCC-SD and Avicel PH-101 showed better thermal stability while Teff straw was highly thermo-resistant above 345 °C (Figure 9). Though little changes are seen in some temperature zones, both TGA (Figure 9) and DTA (Figure 10) thermograms of MCC-SD and Avicel PH-101 showed almost identical pattern in the temperature zone below 400 °C.

Initial weight loss was observed on TGA thermograms of Teff straw (36–117 °C), cellulose (40–108 °C), MCC-SD (41–115 °C) and Avicel PH-101 (38–112 °C) with endothermic peaks on DTA curves (Figure 10) at respective temperatures of 56.84 °C, 64.91 °C, 67.54 °C and 63.59 °C. Their corresponding weight losses were 9.17%, 7.63%, 5.36% and 5.98%, respectively. This weight loss is reported to be associated with evaporation of loosely bound moisture on the surface of the samples and evolution of absorbed water (Adel *et al.*, 2010).

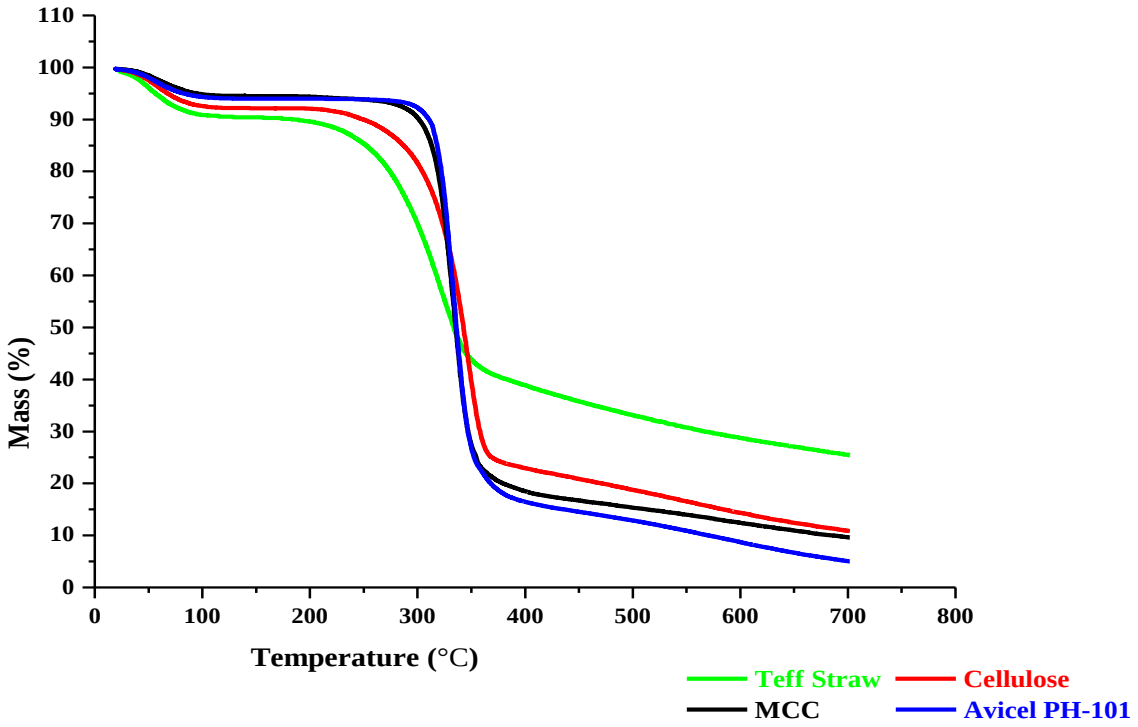

Figure 9: TGA thermograms of raw material, cellulose and MCC samples.

The temperature at which 10% of the material is degraded ($T_{10\%}$) is in increasing order of Teff straw (179.55 °C), cellulose (249.72 °C), MCC-SD (301.41 °C), and Avicel PH-101 (310.67 °C). The degradation of Teff straw on lower temperature is expected to have resulted from thermal depolymerization of hemicellulose and/ or pectin (Jonoobi *et al.,* 2011). Different studies reported that hemicellulose starts to decompose first followed by cellulose which resulted to the evolution of the volatile compounds (Adel *et al.,* 2010). Whereas, lignin is considered to be the most thermo-resistant component of lignocellulosic materials which mainly results in char formation (Ramiah, 1970). Brebu and Vasile (2010) reported that about 40% of lignin remained as residue after heating up to 700 °C. But, presence of high amount of moisture (9.17%) might also have contributed some part for enhanced weight loss of Teff straw. On the other hand, the lower $T_{10\%}$ of MCC-SD compared with Avicel PH-101 might be attributed to its lower degree of crystallinity.

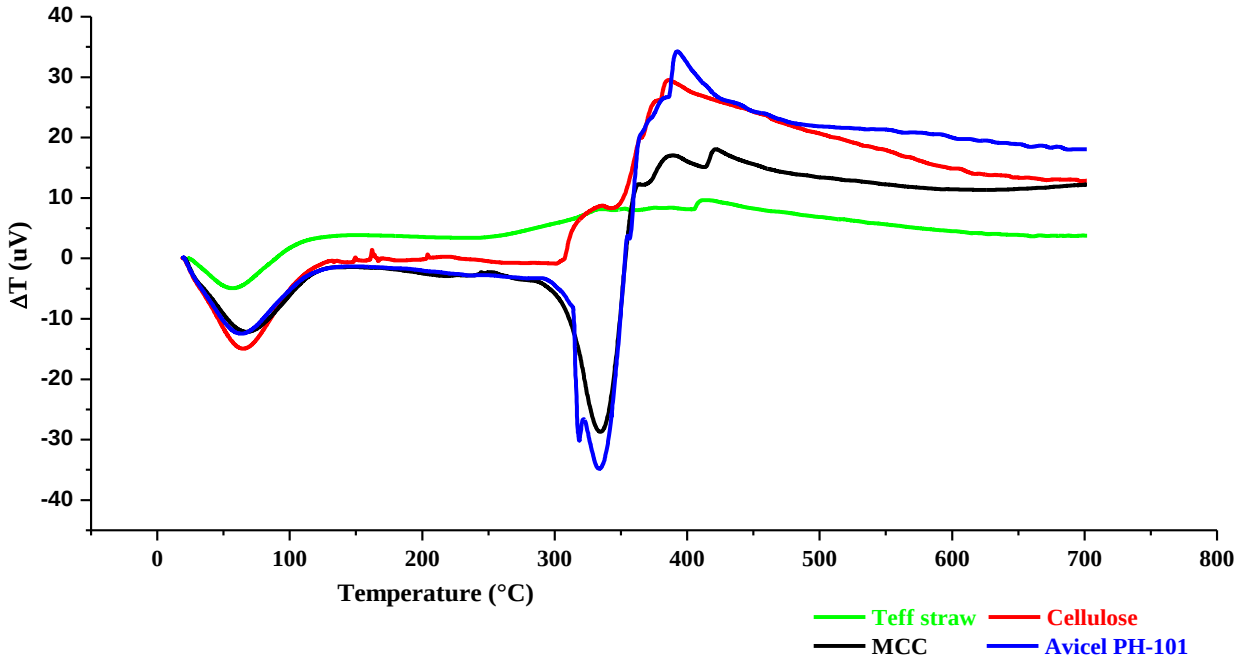

Figure 10: DTA thermograms of raw material, cellulose and MCC samples.

In addition to the initial decomposition, two stages of weight loss are seen in all the samples. During the second stage, rapid degradation was encountered in all the four samples (Figure 10). As can be understood from onset of degradation, thermal stability increases as we go from

raw material (207 °C) through cellulose (232 °C) to MCC (284 °C) and Avicel PH-101 (291 °C). In this stage, higher proportions of all the samples were degraded. MCC-SD and Avicel PH-101 exhibited delayed onset of degradation compared with both cellulose and Teff straw. During this stage, lowest extent of degradation was encountered by Teff straw (49.85%) whereas highest degradation was seen by Avicel PH-101 (75.59%). Also, 68.4% of cellulose and 72.62% of MCC-SD are degraded at this stage. Removal of hemicellulose during cellulose isolation and subsequent reduction of amorphous portions during acid hydrolysis (higher degree of crystallinity thereof) are the main reasons for enhanced stability of Avicel PH-101 (Jonoobi *et al.*, 2011). The relatively earlier onset of major degradation in MCC-SD, compared to Avicel PH-101, could result from its lower degree of crystallinity (Calahorra *et al.*, 1989).

Differences among DTA curves of MCC-SD and Avicel PH-101 are seen on two sites in the major degradation stage (Figure 10). In the first case, temperature change on the endothermic peak at 318.55 °C was higher for Avicel PH-101 (-30.13 uV) than that of MCC-SD (-28.71 uV) at 334 °C. Secondly, a sharp exothermic peak (34.4 uV) was observed at 394 °C from Avicel PH-101 curve whereas lower temperature change was recorded at 397.12 °C (28.68 uV) in case of MCC-SD. The higher extent of degradation of Avicel PH-101 could have consumed more heat and subsequently increased emission of heat. Compounds with higher molecular weight and with even slightly higher amount of impurity will possess increased residue after ignition. Ramiah (1970) reported that DTA curves are very sensitive to presence of small amount of impurities.

Fifty percent of cellulose, MCC-SD and Avicel PH-101 samples were degraded at respective temperatures of 338.98 °C, 335.57 °C and 330.14 °C, whereas Teff straw reached early ($T_{50\%}$ = 324.82 °C). After heating up to 600 °C, residues of Teff straw, cellulose, MCC-SD and Avicel PH-101 were found to be 28.75%, 14.37%, 12.43% and 8.71%, respectively. According to Jahan *et al.* (2011), residue after heating of MCC to similar temperature was found to be 12–14%. Final residue after heating at 700 °C was highest for Teff straw (26.25%) whereas Avicel PH-101 exhibited the lowest (4.99%) value. The analogous values for cellulose and MCC-SD were, respectively, 11.167% and 9.58%. Presence of lignin and its high DP polymers might have contributed for higher temperature resistance at elevated temperature and the high

residue seen in case of Teff straw (Adel *et al.*, 2010; Brebu and Vasile, 2010). According to Yang *et al*. (2007), degradation of lignin displayed not only a wide range of temperature (160–900 °C) but also generated very high amount of solid residue (40%). The higher residue of MCC, compared with Avicel PH-101, could emanate from its higher DP value.

5.2.5. Particle Size and Size Distribution

Among the MCC powders, MCC-0 had significantly higher mean particle size than all the rest MCC powders ($P < 0.05$) (Table 3). Milling of the hydrolyzed cellulose in case of MCC-OD and MCC-SD, and mechanical size reduction after drying of MCC-OD could be the cause for their lower mean particle size compared with MCC-0. At similar confidence level, Avicel PH-101 showed significantly higher mean particle size than both MCC-OD and MCC-SD ($P < 0.05$). Moreover, mean particle size of MCC-OD was significantly lower compared with MCC-SD ($P = 0.009$).

Table 3: Volumetric mean particle size and size distribution of MCC powders (OD = oven dried, SD = spray dried).

Parameters	**Product**			
	MCC-0	MCC-OD	MCC-SD	Avicel PH-101
Mean particle size (µm)	85.89 ± 1.03	45.62 ± 0.91	50.32 ± 1.51	73.81 ± 0.65
Size distribution percentile (µm)				
D(v, 0.1) [14-30]*	10.35 ± 0.1	7.42 ± 0.06	8.49 ± 0.56	19.86 ± 1.77
D(v, 0.2)	20.4 ± 0.23	12.95 ± 0.2	15.90 ± 1.31	31.7 ± 2.03
D(v, 0.5) [40-75]*	59.15 ± 0.85	33.97 ± 0.38	39.34 ± 2.23	61.35 ± 0.61
D(v, 0.8)	148 ± 1.7	71.38 ± 2.69	76.91 ± 2.52	111.4 ± 1.83
D(v, 0.9) [77-156]*	207.4 ± 3.6	100.81 ± 4.37	107.04 ± 1.99	147.77 ± 1.47
Span = [(D(0.9)-(0.1)/D(0.5]	3.332 ± 0.08	2.750 ± 1.44	2.505 ± 0.14	2.085 ± 0.06
Specific surface area (m^2/g)	0.304 ± 0.003	0.285 ± 0.006	0.369 ± 0.007	0.446 ± 0.013

* D(v, X) = represents the size of particles (volume %) below which 'X' fraction of the sample lies.

* The values in parenthesis indicate acceptable range according to manufacturer's specification (Pesonen *et al.*, 1989; Rowe *et al.*, 2009).

Particle size distributions of MCC-OD and MCC-SD differ from that of Avicel PH-101. With the exception of MCC-0, all the MCC powders showed log normal distribution of particle size (Figure 11).

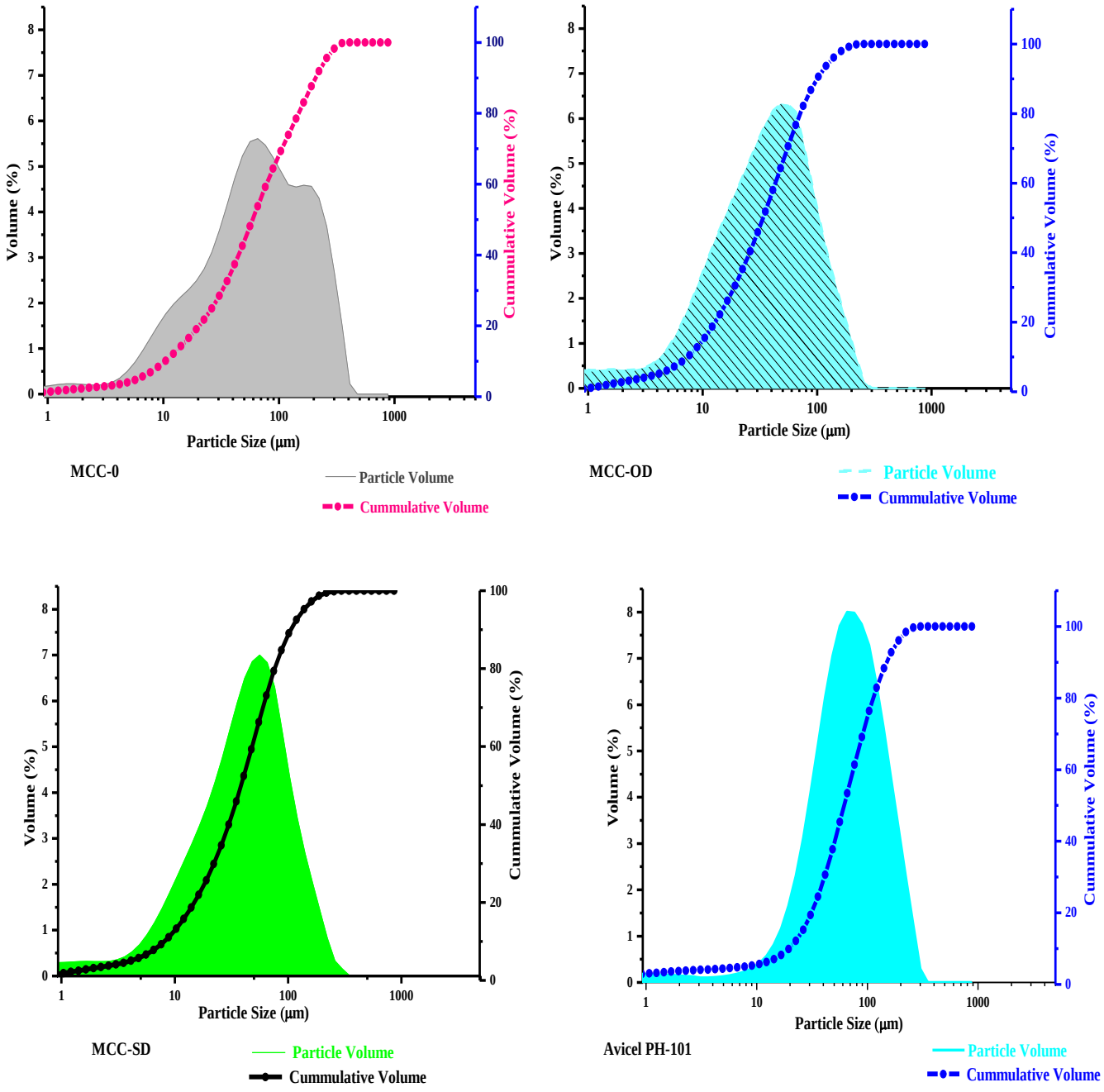

Figure 11: Volume and cumulative volume particle size distributions of MCC powders (OD = oven dried, SD = spray dried).

Avicel PH-101 powder fulfils the three percentile (10, 50 and 90%) acceptable values set by the manufacturer but had higher nominal mean particle size than the reported value of 50 μm. It also had significantly narrower particle size distribution (lower span value) than both MCC-OD (P = 0.002) and MCC-SD (P = 0.007) (Table 3, Figure 11). But there was no statistically significant difference between particle size distributions of MCC-OD and MCC-SD. Whereas MCC-0 displayed the broadest particle size distribution from all the samples. Laser Diffraction defines particle size as the diameter of a sphere with equivalent volume or mass. Hence, the results are better strengthened by other techniques (like microscopy) because it is challenging to accurately measure sizes of particles, like MCC, with higher length-to-width ratio (Malvern operators guide, 1999).

It is reported that specific surface area of Avicel PH-101 is in the range between 1.0 and 1.5 m^2/g (through nitrogen adsorption) and 1.3 m^2/g as determined by mercury porosimetry (Pesonen *et al.*, 1989; Gerad and Arne, 2011). The specific surface area of all MCC powders found in this study are lower than the reported value for Avicel PH-101. This discrepancy could be associated with the limitation of the method used (Laser Diffraction) which underestimates specific surface area because it assumes particles to be spherical in shape and have no or minimum intraparticle porosity (Malvern operators guide, 1999). Specific surface area measured using gas adsorption measures the total free surface of powders including intraparticle space unlike Laser Diffraction which takes the outer surface of particles. Moreover, the higher true density obtained in our study compared with the value reported (1.521g/ml) by Pesonen *et al*. (1989) could have resulted in lower surface area since these variables are inversely related. Surface area of particles which are known to consist largely of irregular particles like MCC (Pesonen *et al.*, 1989) are largely underestimated when Laser Diffraction is used (Bodycomb *et al.*, 2014).

5.2.6. Density and Related Properties

MCC powder is among the commonly used pharmaceutical excipients in solid dosage form manufacturing. It is considered to be the most compactible material (Doelker, 1993) and hence considered as dry binder because it improves the compactibility (tabletability) of the compression mix (Thoorens *et al.*, 2014). Because filler/binder excipients comprise large part

of the compression mix, their powder properties become decisive parameter. Uniformity of blend, die fill and tablet weight are all influenced by powder flow properties.

Flow and compaction properties of powders can be described based on their density profiles. Since the unsettled volume is used for its determination, bulk density depends on both the density of powder particles and the spatial arrangement of particles in the powder bed. It is influenced by the preparation, treatment and storage conditions of the powder. On the other hand, tapped density theoretically indicates the maximum bulk density that can be attained after mechanically tapping of powder without deformation of the particles (USP-30/NF-25–616 (2007). Direct measurement of flow rate of MCC powders, except for the free flowing Avicel PH-200, is not possible unless vibratory hopper techniques are used (Doelker, 1993).

Owing to their simple and fast determination and reliable results, the use of compressibility index and Hausner ratio for predicting powder flow characteristics is becoming common. Compressibility (Carr's) index is influenced by bulk density, size, shape, surface area, moisture content, and cohesiveness of materials. Both compressibility index and Hausner ratio are calculated from bulk density and tapped density of the powder. Using Hausner ratio and Carr's index data, powder flow properties of excipients can be classified as excellent, good, fair, passable, poor, very poor, and very, very poor.

Accordingly, powders are said to have excellent flow if they have Hausner ratio (HR) ≤ 1.11 or compressibility index (CI) of ≤ 10%. Powder flow is assigned as good, fair, passable, poor, very poor and very, very poor for powders which possess HR (CI) of 1.12–1.18 (11–15%), 1.19–1.25 (16–20%), 1.26–1.34 (20–25%), 1.35–1.45 (26–31%), 1.46–1.59 (32–37%) and > 1.6 (> 38%), respectively (USP-30/NF-25–1174 (2007)).

Density and related properties of the prepared MCC and Avicel PH-101 powders are summarized in Table 4. MCC-OD and Avicel PH-101 displayed comparable values of both bulk and tapped density. MCC-0 had significantly lower bulk density than the rest MCC powders. The decrease in bulk and tapped density in case of MCC-SD, compared with MCC-OD, could result from the fact that porosity increases with spray drying (Thoorens *et al.,* 2014). MCC-SD showed significantly higher porosity value than both MCC-OD and Avicel PH-101.

However, this increased porosity will improve compactibility of the powder resulting in tablets with higher strength (Kumar *et al.*, 2002). Moreover, the lower moisture content will also play some role in the higher bulk and tapped density of MCC-OD (Amidon and Houghton, 1995).

Table 4: Density and related properties of MCC powders (OD = oven dried, SD = spray dried).

Property	Product			
	MCC-0	**MCC-OD**	**MCC-SD**	**Avicel PH-101**
Density (g/cm^3)				
Bulk	0.143 ± 0.001	0.344 ± 0.002	0.25 ± 0.03	0.348 ± 0.001
Tapped	0.216 ± 0.001	0.457 ± 0.003	0.353 ± 0.01	0.461 ± 0.0003
True	1.555 ± 0.005	1.552 ± 0.01	1.556 ± 0.05	1.564 ± 0.002
Porosity (%)	90.15 ± 0.12	77.86 ± 0.12	83.93 ± 0.12	77.78 ± 0.28
Carr's Index (%)	33.86 ± 0.15	24.81 ± 0.49	29.16 ± 0.14	24.56 ± 0.14
Hausner Ratio	1.51 ± 0.012	1.33 ± 0.008	1.41 ± 0.003	1.32 ± 0.003

MCC-OD and Avicel PH-101 showed passable flow property, while MCC-SD had poor flow. Due to its very poor flow property (CI = 33.86%), MCC-0 was excluded from tablet studies. The narrow particle size distribution along with its larger mean particle size (Section 5.2.5) could make Avicel PH-101 to have better flow property than MCC-SD (Pesonen and Paronen, 1986). There was no statistically significant difference in true density of all the prepared and commercial MCC powders. True densities of all samples were in agreement with commonly reported value (1.512 g/cm^3 to 1.668 g/cm^3) for MCC powder (Rowe *et al.*, 2009).

5.2.7. Moisture Sorption

Moisture is known to affect the mechanical properties and functionalities of powders. Storage of MCC powder at elevated humidity conditions results in decreased bulk density and hence adversely affects its compaction properties (Williams *et al.*, 1997). Amorphous portion of MCC is considered to be responsible for moisture absorption, hence increased degree of crystallinity will result in lower moisture absorption (Nokhodchi, 2005).

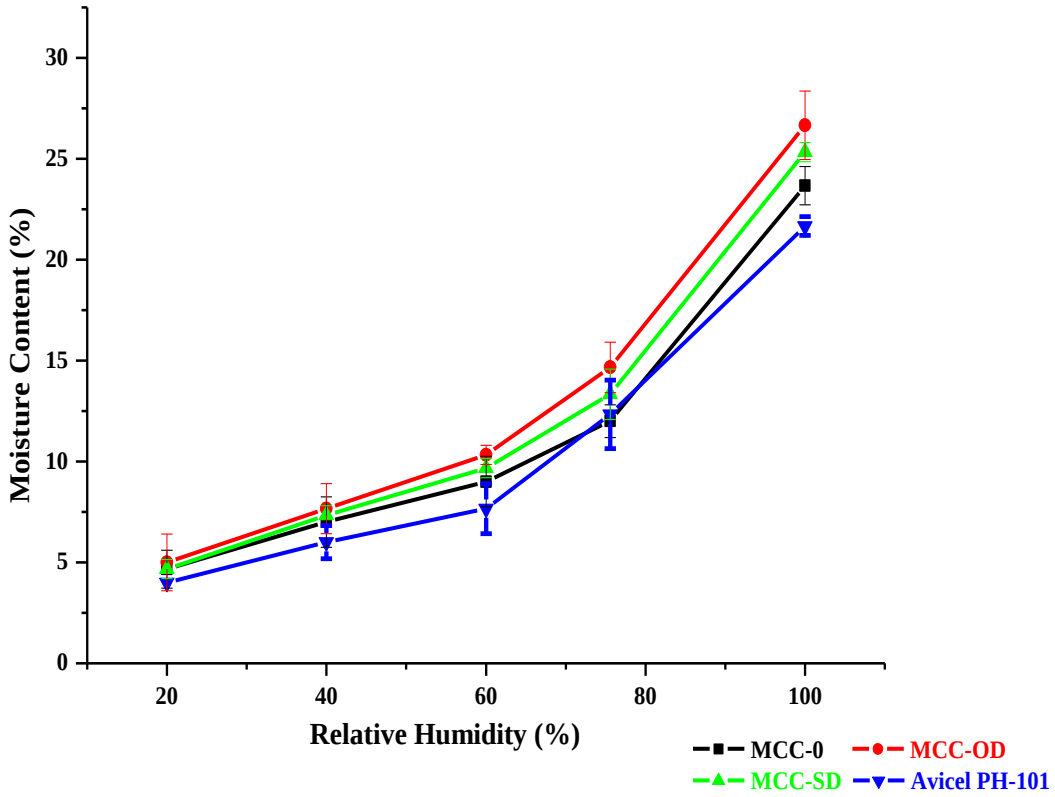

Figure 12: Moisture sorption patterns of the prepared and commercial MCC powders (n = 3, mean ± SD) (OD = oven dried, SD = spray dried).

MCC-OD, which has the lowest degree of crystallinity, displayed highest moisture absorption at all levels of relative humidity. The relative stability of Avicel PH-101 could emanate from its high degree of crystallinity (Table 2). Above 40% RH, moisture contents of samples exceeded the acceptable limit set for MCC (≤ 7%) (BP, 2009) which may affect powder flow, compressibility and tablet strength. Significant changes in compressibility index, and in tableting and mechanical properties of MCC are reported at respective moisture contents of above 6% and 5% (Amidon and Houghton, 1995). This phenomenon is believed to be associated with the plasticizing effect of water which renders the macromolecules less rigid and facilitates the slippage and flow of individual microcrystals (Doelker, 1993).

Extensive moisture absorption is encountered at higher RH values (RH > 60%). Hence, humidity of storage and operation conditions of these MCC powders needs to be monitored in order not to hinder the powder and tablet properties (Sun, 2008). On the other hand, the high

moisture sorption property of MCC powder along with its high porosity promotes swelling and disintegration of MCC tablets (Thoorens *et al.*, 2014). Hence, these properties of MCC powder could make it good candidate to be used as disintegrating agent.

5.3. Evaluation of Tablet Properties

5.3.1. Lubricant Sensitivity Ratio

Products which have Lubricant Sensitivity Ratio (LSR) values close to unity are considered highly sensitive to the lubricant used. Crushing/tensile strength reduction was observed in compacts of all the MCC powders upon addition of magnesium stearate (0.5%). The decrease in tablet strength has been attributed to formation of weaker bonds, after compression, between lubricant-lubricant molecules rather than strong excipient-excipient bonds (Gerard and Hans, 2011). As presented by Table 5, LSR of MCC powders was in the order of Avicel PH-101 > MCC-OD > MCC-SD. LSR is largely determined by the completeness of the lubricant surface film formation which depends on both flow property and surface area of MCC powder (Doelker *et al.*, 1995).

Table 5: Impact of addition of magnesium stearate (0.5%) on hardness of tablets compressed from plain MCC powders (OD = oven dried, SD = spray dried).

Product	**Hardness (N)**		**LSR**
	Plain	**Lubricated**	
MCC-OD	49.83 ± 2.40	41.83 ± 1.94	0.16 ± 0.008
MCC-SD	68.65 ± 1.56	59.05 ± 1.12	0.14 ± 0.012
Avicel PH-101	116.67 ± 4.08	94.33 ± 3.20	0.19 ± 0.010

Particle size is reported to affect flow and surface area available for the lubricant whereas moisture content affects flow and the magnitude and nature of the attractive forces between excipient and the lubricant. A decrease in both particle size and flowability results in decreased influence of lubricants (Vromans *et al.*, 1988). The poor flow property of MCC-SD could hinder mixing with the lubricant and hence reduced its sensitivity. The higher specific surface area of Avicel PH-101, in addition to its better flow property, could make it to be the most

sensitive for magnesium stearate lubrication. The LSR values obtained in this study are larger than those reported by Doelker *et al*. (1995). The Avicel PH-101 powder they used, however, had lower mean particle size (50 μm) and inferior flow (HR = 1.57) property than the one used in our study which could bring about this discrepancy. Moreover, they mixed the lubricant and MCC powders for 5 min at 25 rpm. Whereas, mixing was conducted for similar duration but at 45 rpm in our study. Bolhuis *et al*. (1987) confirmed that rotation speed of mixers has considerable impact on tablet hardness of lubricated powders.

5.3.2. Tablets Compressed from Plain MCC Powders

5.3.2.1. Weight, Thickness and Diameter

The weight, thickness and diameter of tablets prepared from plain MCC powders are presented in Table 6. Though fixed die volume was used which can accommodate 400 mg of the MCC powders, MCC-SD tablets prepared at all compression forces had significantly lower weight than their analogous tablets of both MCC-OD and Avicel PH-101 ($P < 0.05$) powders.

Table 6: Weight, thickness and diameter of tablets compressed from plain MCC powders at different compression forces (OD = oven dried, SD = spray dried).

Product	**Parameter**	**Compression Force**				
		CF1	**CF2**	**CF3**	**CF4**	**CF5**
MCC-OD	Weight (mg)	385 (3.1)	385 (2.31)	383 (4.5)	386 (5.2)	388 (8.2)
	Thickness (mm)	6.35 (0.01)	5.91 (0.02)	5.53 (0.02)	5.34 (0.01)	4.97 (0.01)
	Diameter (mm)	*	10.92 (0.01)	10.89 (0.01)	10.94 (0.01)	10.91 (0.01)
MCC-SD	Weight (mg)	378 (3.7)	378 (5.4)	362 (7.9)	364 (7.2)	358 (10.3)
	Thickness (mm)	6.65 (0.04)	6.14 (0.16)	5.77 (0.01)	5.57 (0.01)	5.15 (0.02)
	Diameter (mm)	10.93 (0.03)	10.91 (0.02)	10.90 (0.01)	10.92 (0.01)	10.90 (0.02)
Avicel PH-101	Weight (mg)	402 (0.3)	399 (1.2)	398 (1.5)	398 (2.4)	401 (1.1)
	Thickness (mm)	6.39 (0.03)	5.91 (0.03)	5.58 (0.02)	5.30 (0.01)	5.0 (0.01)
	Diameter (mm)	10.90 (0.01)	10.90 (0.01)	10.88 (0.03)	10.91 (0.01)	10.88 (0.01)

* The values in parenthesis indicate standard deviation. * = tablets broke during test.

* CF = target hardness of Avicel PH-101 tablet: 50N (CF1), 75N (CF2), 100N (CF3), 125N (CF4) & 150N (CF5).

There also exists statistically significant weight difference between MCC-OD and Avicel PH-101 tablets. This weight difference could have resulted from variation in bulk density of the powders. Weight variation of tablets of all the three MCC powders prepared at all compression forces falls within acceptable range of weight variation (± 5%) for tablets weighing 250 mg or more (BP, 2009). However, we cannot conclude that these MCC powders have no problem in flowability since separately weighed compression mass was hand-filled into the die before each compression. Tablet thickness decreased with increasing compression force in all MCC samples. Moreover, thickness of MCC-SD tablets was significantly higher than those of MCC-OD and Avicel PH-101 tablets prepared at all compression forces.

5.3.2.2. Crushing Strength, Tensile Strength and Friability

Statistically significant (CI = 95%) difference in crushing strength was observed between MCC-OD and MCC-SD tablets at low (CF2) and high (CF5) compression forces (Figure 13).

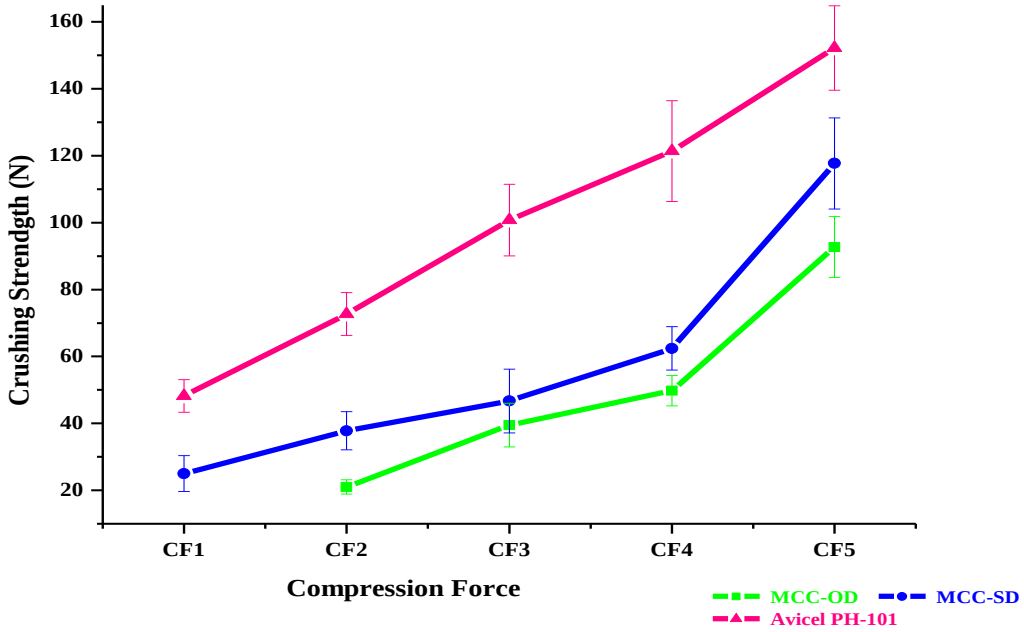

Figure 13: Crushing strength of tablets prepared from plain MCC powders at different compression forces (n = 10, mean ± SD) (OD = oven dried, SD = spray dried).

* CF is the compression force adjusted to give Avicel PH-101 tablets with hardness of 50N (CF1), 75N (CF2), 100N (CF3), 125N (CF4), & 150N (CF5).

Tablets prepared from plain MCC-OD and MCC-SD at all compression forces (CF1-CF5) showed significantly lower crushing strength than those of Avicel PH-101 ($P < 0.05$). Tensile strength and friability of tablets prepared from plain MCC powders are summarized in Table 7. At all compression forces, Avicel PH-101 tablets displayed significantly higher tensile strength than both MCC-SD and MCC-OD tablets. Moreover, tensile strengths of MCC-SD tablets compressed at CF2 and CF5 were found to be significantly higher than MCC-OD tablets compressed with similar forces. The higher specific surface area of MCC-SD and Avicel PH-101 (Section 5.2.5), compared to MCC-OD, could have improved their compactibility. Additionally, the higher degree of crystallinity of MCC-SD and Avicel PH-101 powders (Section 5.2.3) could have resulted in higher tablet strength than MCC-OD which had significantly lower degree of crystallinity (Suzuki and Nakagami, 1999). The variation in degree of crystallinity and specific surface area could also be reasoned out for the observed difference in hardness between tablets of MCC-SD and Avicel PH-101.

Table 7: Tensile strength, friability and disintegration time of tablets compressed from plain MCC powders at different compression forces (OD = oven dried, SD = spray dried).

Product	**Parameter**	**Compression Force**				
		CF1	**CF2**	**CF3**	**CF4**	**CF5**
MCC-OD	Tensile strength ($Kgcm^{-2}$)	*	2.11 ± 0.23	4.26 ± 0.69	5.53 ± 0.51	11.09 ± 1.12
	Friability (%)	*	0.95	0.62	0.37	0.24
	Disintegration time (min)	#	#	0.65 ± 0.07	1.42 ± 0.1	5.15 ± 1.02
MCC-SD	Tensile strength ($Kgcm^{-2}$)	2.42 ± 0.41	3.89 ± 0.55	4.81 ± 0.93	6.66 ± 0.66	13.60 ± 1.55
	Friability (%)	0.78	0.71	0.52	0.34	0.13
	Disintegration time (min)	#	0.68 ± 0.05	1.26 ± 0.72	2.18 ± 0.13	6.36 ± 1.24
Avicel PH-101	Tensile strength ($Kgcm^{-2}$)	4.87 ± 0.48	7.42 ± 0.64	10.77 ± 1.02	13.85 ± 1.68	18.15 ± 1.48
	Friability (%)	0.48	0.23	0.18	0.11	0.05
	Disintegration time (min)	0.58 ± 0.01	0.72 ± 0.03	1.37 ± 0.64	3.61 ± 0.21	7.05 ± 1.35

* = Tablets broke during test; # = Not determined.

* CF represents compression force adjusted to give Avicel PH-101 tablets with hardness of 50N (CF1), 75N (CF2), 100N (CF3), 125N (CF4), & 150N (CF5).

With the exception of those compressed from MCC-OD at CF1, all the prepared tablets had friability values in the acceptable range (<1%). Friability of tablets prepared from all the three powders decreased, obviously, with increasing compression force. There was marked difference in friability profile between tablets compressed from various plain MCC powders at similar compression force.

5.3.2.3. Disintegration Time

Disintegration time of tablets compressed from plain MCC tablets is presented in Table 7. The disintegration time of all the three products increases with tablet hardness. Although Avicel PH-101 tablets showed higher crushing strength than both MCC-SD and MCC-OD tablets, early disintegration was encountered. This faster disintegration might be ascribed to the higher specific surface area of Avicel PH-101 powder. Since disintegration of MCC tablets is attributed to the penetration of water into the hydrophilic tablet matrix by means of capillary action of the pores (Gerard and Arne, 2011), the relatively higher amount of residual wax found in MCC-OD and MCC-SD might have slowed their swelling. Moreover, the lower hydration capacity, which results in lower swelling capacity, could also have increased disintegration times of MCC-OD and MCC-SD (Rojas and Kumar, 2011).

5.3.3. Tablets Compressed from MCC Powders Loaded with Paracetamol

5.3.3.1. Weight, Thickness and Diameter

As can be seen from Table 8, weight variations of tablets prepared from all the three MCC powders at all paracetamol concentrations fall within acceptable range of weight variation (< 5%) for tablets weighing 250 mg or more (BP, 2009). Based solely on this result, however, it is difficult to conclude that the excipients used in this study confirm content uniformity of blend because the weighed powder mass was hand-filled before each tablet was compressed. There was no statistically significant difference in thickness and diameter of tablets prepared with similar concentration of drug from all the three MCC powders.

Table 8: Properties of tablets compressed from MCC powders loaded with different percentages of paracetamol (OD = oven dried, SD = spray dried).

Product	Parameter	Paracetamol Content (Weight %)			
		30	45	60	75
MCC-OD	Weight (mg)	380.3 ± 9.6	381.5 ± 18.5	377.4 ± 6.2	375.3 ± 8.6
	Thickness (mm)	4.93 ± 0.05	4.96 ± 0.02	4.96 ± 0.06	5.03 ± 0.05
	Diameter (mm)	10.92 ± 0.01	10.92 ± 0.01	10.93 ± 0.01	10.91 ± 0.01
	Hardness (N)	45.7 ± 6.3	33.5 ± 1.7	24.3 ± 2.5	16.7 ± 3.9
	Friability (%)	0.495	0.736	1.873	*
	Disintegration time (Min)	1.68 ± 0.3	1.08 ± 0.1	#	#
MCC-SD	Weight (mg)	384 ± 12.4	381.6 ± 12.9	379.3 ± 13.9	378.8 ± 6.6
	Thickness (mm)	4.88 ± 0.05	4.91 ± 0.05	4.92 ± 0.04	4.97 ± 0.05
	Diameter (mm)	10.92 ± 0.03	10.93 ± 0.02	10.93 ± 0.01	10.90 ± 0.01
	Hardness (N)	68.5 ± 8.2	44.5 ± 4.3	34 ± 3.8	26.5 ± 4.7
	Friability (%)	0.326	0.603	0.852	1.345
	Disintegration time (Min)	2.47 ± 0.4	1.67 ± 0.2	1.19 ± 0.1	#
Avicel PH-101	Weight (mg)	389.6 ± 9.6	380.6 ± 15.1	377.8 ± 6.2	374.2 ± 4.3
	Thickness (mm)	4.87 ± 0.05	4.87 ± 0.05	4.91 ± 0.02	4.93 ± 0.03
	Diameter (mm)	10.91 ± 0.01	10.92 ± 0.01	10.93 ± 0.03	10.92 ± 0.01
	Hardness (N)	80.7 ± 8.6	58.8 ± 9.5	35.6 ± 8.2	25.8 ± 1.7
	Friability (%)	0.103	0.411	0.795	1.571
	Disintegration time (Min)	2.23 ± 0.4	1.44 ± 0.1	0.83 ± 0	#

* = Tablets broke during test.

= Not determined.

5.3.3.2. Crushing Strength, Tensile Strength and Friability

The diametrical crushing strength and friability of paracetamol loaded (30-75%) MCC tablets are summarized in Table 8 while their tensile strength is illustrated in Figure 14. At all levels of paracetamol concentration, tablets prepared from MCC-OD showed significantly lower crushing strength than those of MCC-SD and Avicel PH-101 (except at 60%). Though not

statistically significant, MCC-SD tablets showed lower crushing strength than Avicel PH-101 at 30 & 45% paracetamol. But at higher paracetamol concentrations (60 and 75%), MCC-SD and Avicel PH- 101 tablets exhibited comparable crushing strengths.

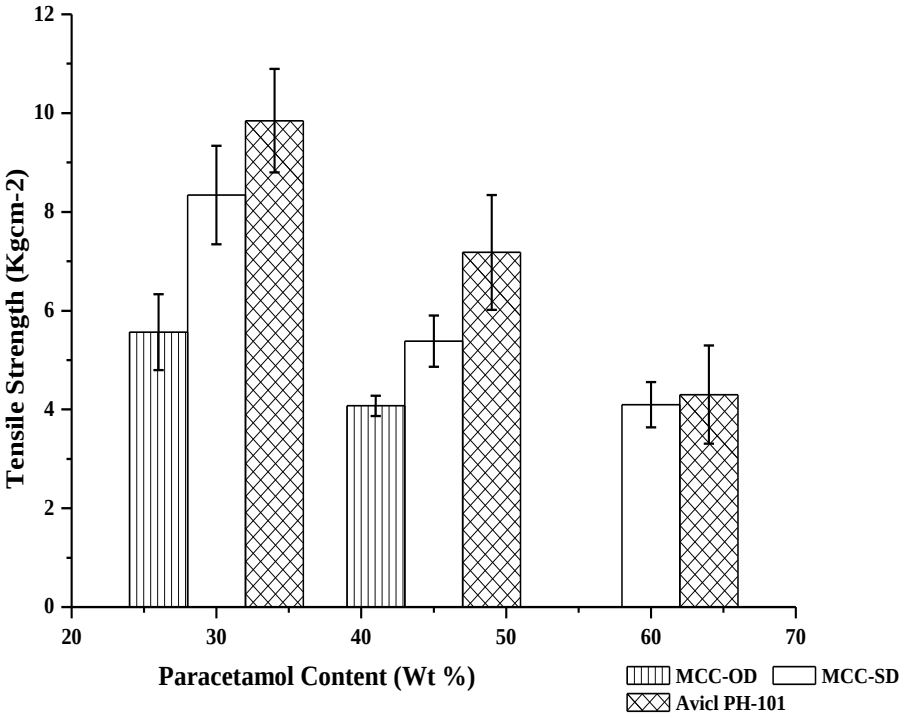

Figure 14: Tensile strength of tablets compressed from MCC powders with different Paracetamol loading (n = 10, mean ± SD) (OD = oven dried, SD = spray dried).

There was no statistically significant difference in tensile strengths between MCC-SD and Avicel PH-101 tablets at all levels of drug loading. Tablets prepared from MCC-OD, however, showed significantly lower tensile strength than Avicel PH-101 at 30, 45 and 75% paracetamol. MCC-OD tablets also exhibited significantly lower tensile strength than MCC-SD tablets at all levels of drug loading. According to the present study, the friability of paracetamol tablets containing MCC-SD and Avicel PH-101 were in the acceptable range (< 1%) (USP30-NF25) with the exception of tablets with 75% drug content. Whereas, tablets compressed from MCC-OD with only 30 or 45% paracetamol loading had friability values in the acceptable range.

5.3.3.3. Dilution Capacity

Dilution capacity represents the maximum percentage of active ingredient that can be loaded to produce tablets with acceptable hardness. Dilution capacity of Avicel PH-101, using paracetamol as model drug, was reported to be 79.9% (w/w) (Kuentz and Leuenberger, 2000). A lower dilution capacity of Avicel PH-101 (65%) was reported by previous study using similar model drug (Habib *et al.,* 1996). Looking at the tensile strength values found in this study, we can say that MCC-SD and Avicel PH-101 have closely related dilution capacity for the model drug used. Hence, equivalent amount of paracetamol reported for Avicel PH-101 in various literatures can be loaded with MCC-SD provided that compression pressures are adjusted for itself. But, MCC-OD exhibited lower dilution potential compared with both MCC-SD and Avicel PH-101 (Figure 14).

5.3.3.4. Disintegration Time

All paracetamol loaded MCC tablets had disintegration time of less than 15 min which is recommended for conventional dosage forms. Tablets prepared from MCC-SD showed delayed disintegration than MCC-OD and Avicel PH-101 tablets with equivalent hardness. Differences in particle specific surface area and hydration capacity could have resulted in the variations between disintegration times of these tablets (Gerard and Arne, 2011; Rojas and Kumar, 2011).

5.3.3.5. *In-Vitro* Drug Release Study

The absorbance (at 243 nm) versus concentration plot prepared from paracetamol solutions gave a linear regression equation $Y = 0.5702X - 0.02881$ (where Y is the absorbance and X is the concentration in µg/mL) and correlation coefficient, $R^2 = 0.999$ (Figure 15).

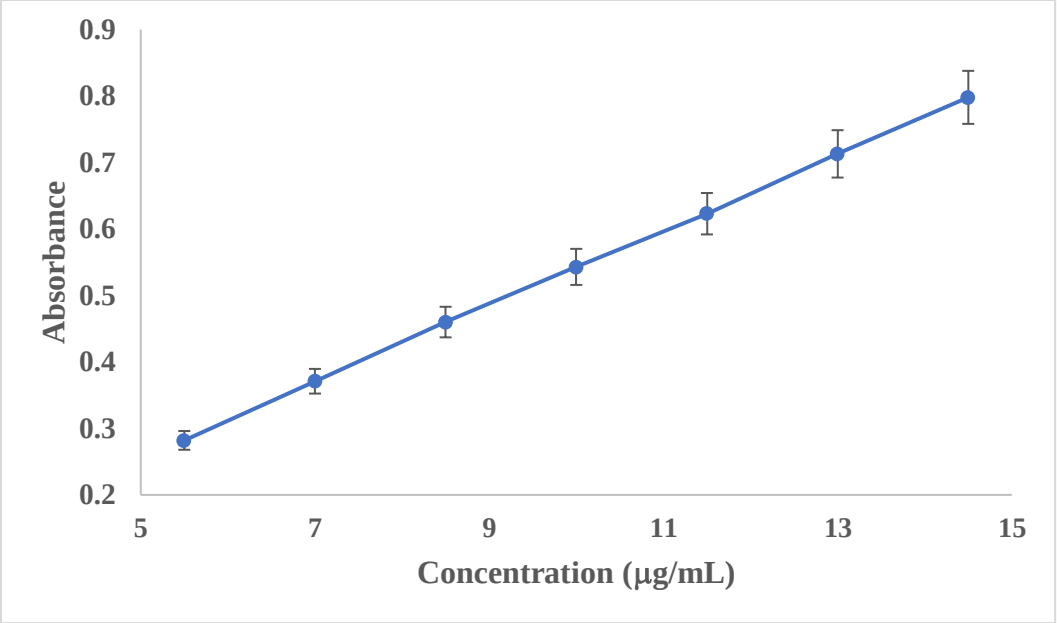

Figure 15: UV Calibration curve of paracetamol standard in pH 5.8 phosphate buffer at 243 nm with 95% confidence interval (R^2 = 0.999).

Dissolution profiles of the selected formulations are illustrated in Figure 16 and summarized in Table 9. All the formulations displayed dissolution profile which is in agreement with the pharmacopoeial limit set for conventional tablets (USP30-NF25). There was no significant difference in dissolution profiles of paracetamol tablets prepared from all MCC powders. Though not statistically significant, tablets with high paracetamol content seemed to dissolve faster in the first five minutes. This could be encountered due to differences in hardness and disintegration time.

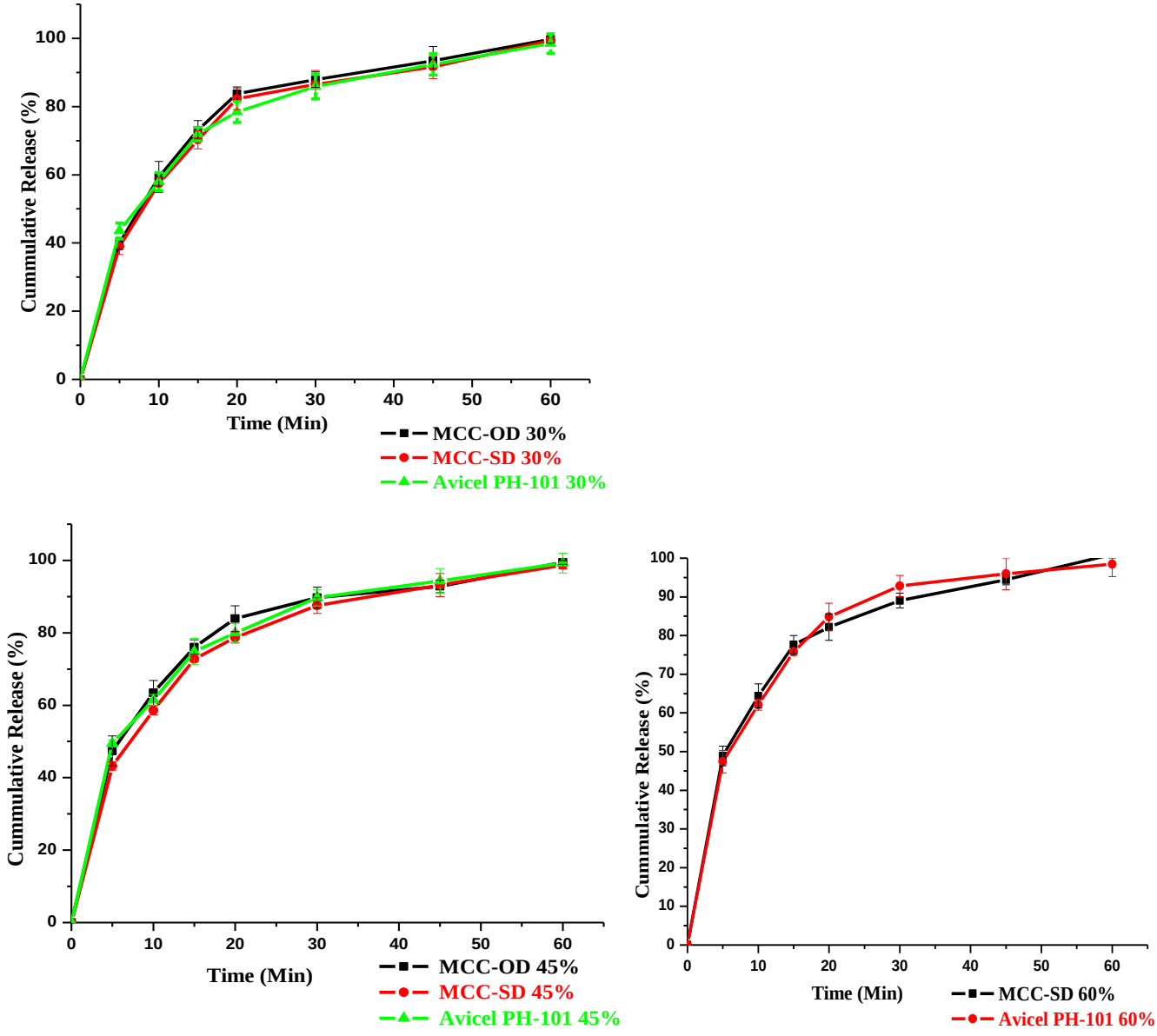

Figure 16: Dissolution profiles of paracetamol loaded MCC tablets (OD = oven dried, SD = spray dried).

Table 9: Dissolution profiles of paracetamol loaded MCC tablets (OD = oven dried, SD = spray dried).

Product (PCM content)	Drug released (%) at each sampling time (Min)						
	5	10	15	20	30	45	60
MCC-OD (30%)	39.86 (1.73)	59.38 (4.52)	73.08 (2.84)	83.82 (1.96)	87.90 (2.28)	93.46 (4.17)	99.72 (1.04)
MCC-SD (30%)	38.99 (2.38)	57.39 (1.92)	70.26 (2.64)	82.28 (3.16)	86.50 (4.07)	91.59 (3.35)	99.40 (0.81)
Avicel PH-101 (30%)	43.55 (2.35)	58.02 (2.65)	71.93 (1.92)	78.41 (3.08)	85.89 (3.68)	92.37 (3.15)	98.48 (2.87)
MCC-OD (45%)	47.36 (4.15)	63.42 (3.46)	76.05 (2.02)	83.93 (3.53)	89.71 (2.95)	92.82 (1.73)	99.43 (0.54)
MCC-SD (45%)	43.21 (1.16)	58.64 (1.24)	72.77 (0.81)	78.71 (1.53)	87.55 (2.17)	93.17 (3.21)	98.73 (1.04)
Avicel PH-101 (45%)	49.49 (0.97)	61.50 (1.46)	74.83 (3.65)	79.96 (2.54)	89.70 (2.27)	94.34 (3.43)	99.26 (2.71)
MCC-SD (60%)	48.88 (2.52)	64.38 (3.14)	77.62 (2.38)	82.17 (3.42)	89.03 (1.93)	94.41 (1.28)	101.0 (0.64)
Avicel PH-101 (60%)	47.41 (2.91)	62.12 (1.39)	75.80 (0.90)	84.86 (3.48)	92.81 (2.73)	95.95 (4.09)	98.43 (3.17)

* The values in parenthesis indicate standard deviation.

5.4. Drug-Excipient Compatibility Study

The IR spectra of paracetamol powder (Figure 17) and its one-to-one mixture with the prepared MCC powder (Figure 18) are presented below. In both figures, the sharp peak at 3321 represents N-H stretching while the broad peak at similar position shows presence of O-H stretching. Stronger bands above 2800 cm^{-1} are attributed to the stretching vibrations of the methyl groups of both paracetamol and MCC. On the other hand, C=O stretching of the carboxyl ion of paracetamol was reflected by a peak at 1651 cm^{-1} in both pure drug and the powder mixture. The band at 1562 cm^{-1}, which is characteristic of C=C stretching of paracetamol (Burgina *et al.*, 2004; Zaki, 2011), is also seen in both figures. Except for O-H stretching, the other characteristic IR bands of paracetamol are not, moreover, found in MCC IR spectrum (Section 5.2.2). Furthermore, the characteristic IR bands of MCC (Figure 6) are also observed in the spectrum of the powder mixture. Since characteristic peaks of both paracetamol and MCC are reflected on the spectrum of the powder mixture, no incompatibility issue is anticipated.

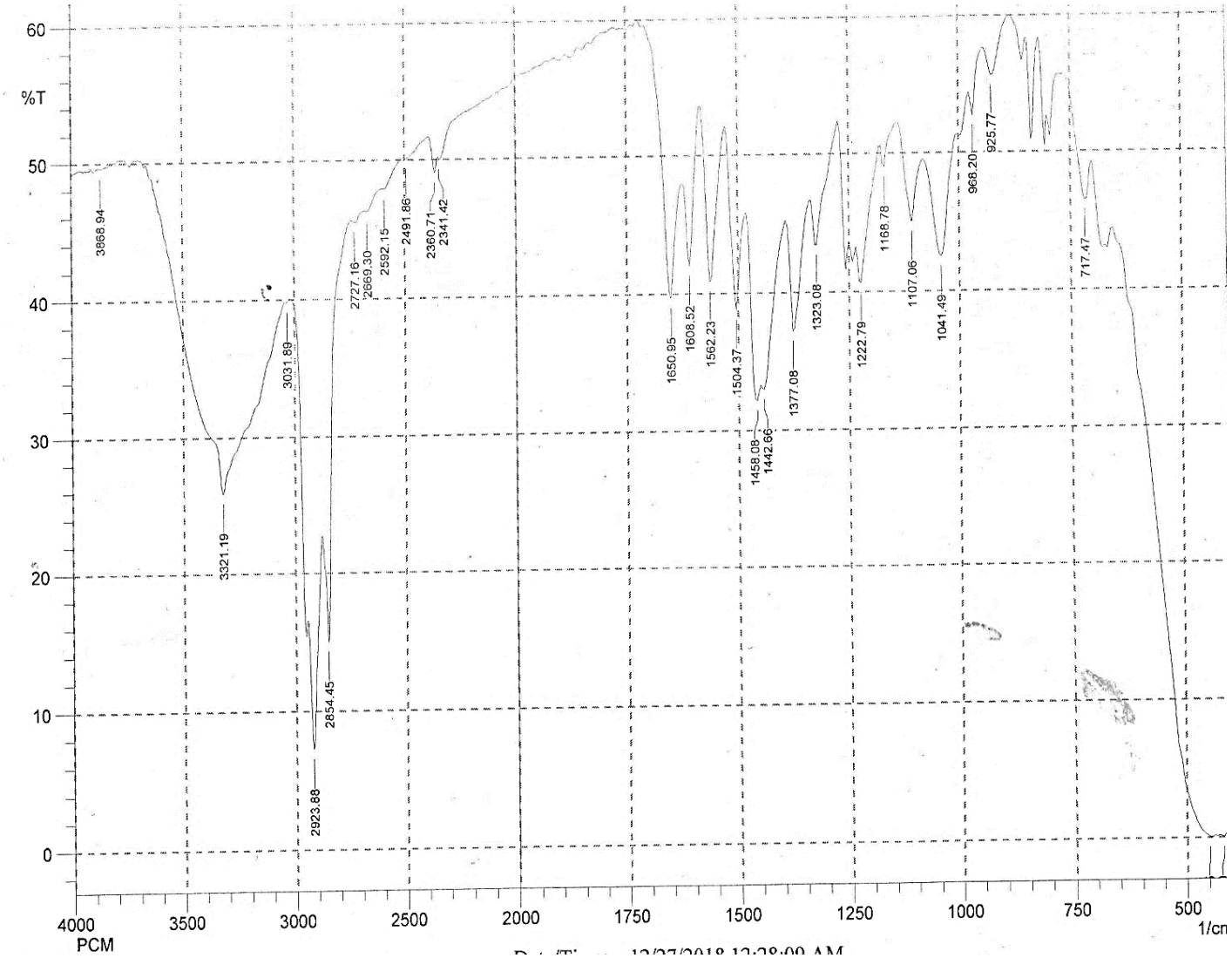

Figure 17: Infrared spectrum of paracetamol powder.

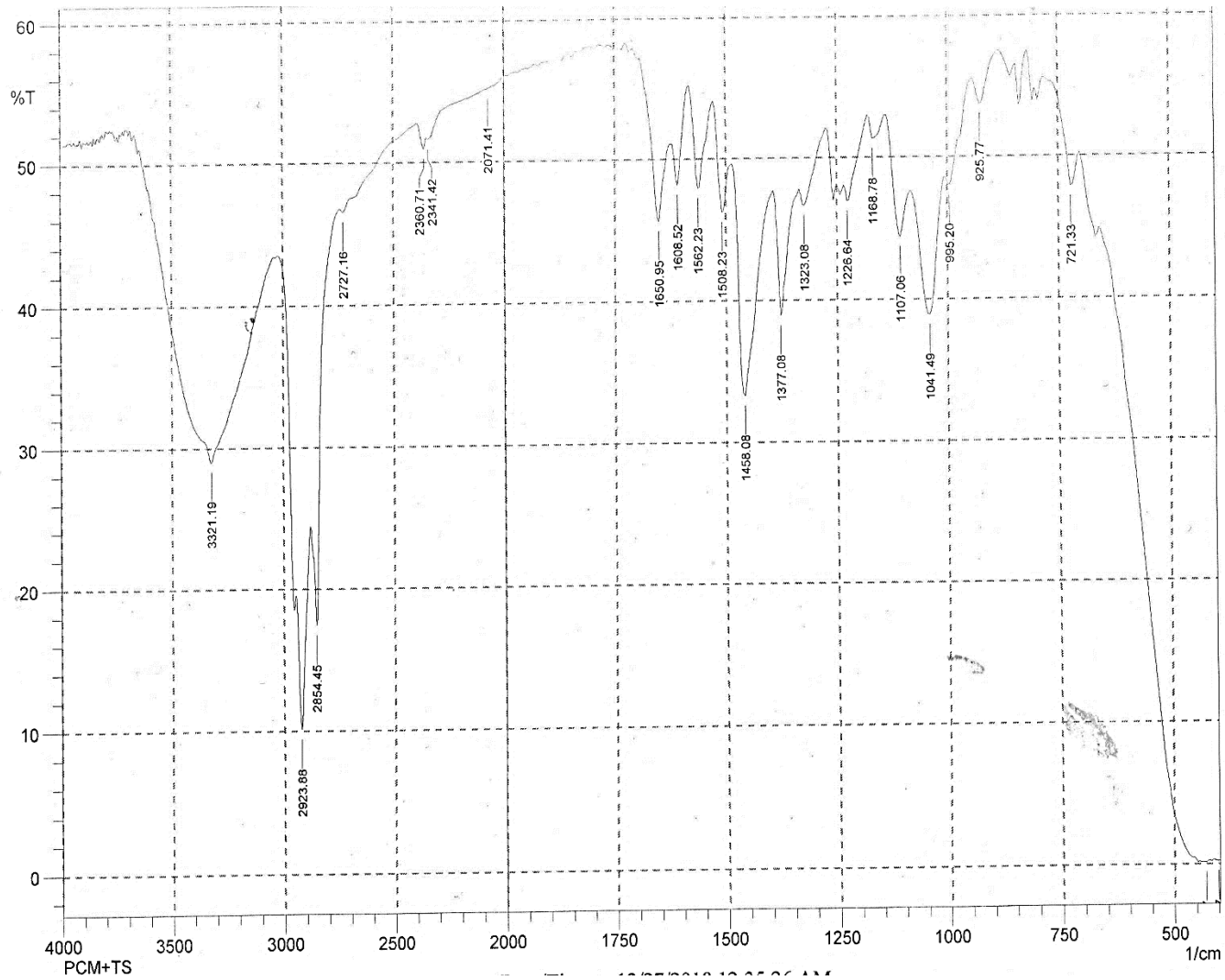

Figure 18: Infrared spectrum of one-to-one mixture of paracetamol and MCC-SD powders.

6. CONCLUSION

Cellulose was effectively isolated from Teff straw through acid-based treatment with comparable yield to commonly reported values in the literature. The isolated cellulose was characterized with SEM, FTIR, XRD, TGA & DTA. Both degree of crystallinity and crystal size were increased with HCl catalyzed hydrolysis of the isolated cellulose. The density, mean particle size and particle size distribution of both MCC-SD and MCC-OD agreed with the values set for Avicel PH-101. Although MCC-SD showed lower compressibility than Avicel PH-101 when compressed alone, their paracetamol formulations had comparable tablet properties. But paracetamol loaded MCC-OD tablets showed inferior tablet tensile strength and hence lower dilution potential. The prepared MCC powders showed better tolerance for lubrication with magnesium stearate than Avicel PH-101. Paracetamol loaded MCC tablets exhibited acceptable in-vitro drug release properties. Taking into consideration that the isolated MCC powder fulfils most of the required characteristics for pharmaceutical applications; and the availability of large amount of Teff straw as byproduct, it may be concluded that the straw can be considered as promising alternative source of MCC. However, the flow property of MCC powders prepared from this straw should be improved.

7. SUGGESTIONS FOR FURTHER WORK

The followings are suggested for further investigation:

- Optimization of MCC preparation processes (like hydrolysis conditions, post hydrolysis milling and spray drying variables).
- Long- and short-term stability studies of tablets compressed from the prepared MCC powder.

REFERENCES

Abule, E., Umunna, N.N., Nsahlai, I.V., Osuji, P.O. and Alemu, Y., 1995. The effect of supplementing Teff (Eragrostis tef) straw with graded levels of cowpea (Vigna unguiculata) and lablab (Lablab purpureus) hays on degradation, rumen particulate passage and intake by crossbred (Friesian× Boran (zebu)) calves. *Livestock Prod. Sci.* **44**: 221–228.

Adel, A.M., El–Wahab, Z.H.A., Ibrahim, A.A. and Al-Shemy, M.T., 2010. Characterization of microcrystalline cellulose prepared from lignocellulosic materials. Part I. Acid catalyzed hydrolysis. *Bioresour. Technol*. **101**: 4446–4455.

Adel, A.M., El–Wahab, Z.H.A., Ibrahim, A.A. and Al-Shemy, M.T., 2011. Characterization of microcrystalline cellulose prepared from lignocellulosic materials. Part II: Physicochemical properties. *Carbohydr. Polym.* **83**: 676–687.

Adler, E., 1977. Lignin chemistry-past, present and future. *Wood Sci. Technol.* **11**: 169–218.

Agarwal, U.P., Ralph, S.A., Baez, C., Reiner, R.S. and Verrill, S.P., 2017. Effect of sample moisture content on XRD-estimated cellulose crystallinity index and crystallite size. *Cellulose*, **24**: 1971–1984.

Alemdar, A. and Sain, M., 2008. Isolation and characterization of nanofibers from agricultural residues-Wheat straw and soy hulls. *Bioresour. Technol*. **99**:1664–1671.

Amidon, G.E. and Houghton, M.E., 1995. The effect of moisture on the mechanical and powder flow properties of microcrystalline cellulose. *Pharm. Res.* **12**: 923–929.

ASTM D1348-94(2003). Standard Test Methods for Moisture in Cellulose. ASTM International, West Conshohocken, PA, 2003.

Barros, J., Serk, H., Granlund, I. and Pesquet, E., 2015. The cell biology of lignification in higher plants. *Ann. Bot.* **115**: 1053–1074.

Battista, O.A. and Smith, P.A., 1962. Microcrystalline cellulose. *Ind. Eng. Chem.* **54**: 20–29.

Battista, O.A., 1950. Hydrolysis and crystallization of cellulose. *Ind. Eng. Chem.* **42**: 502–507.

Battista, O.A., Coppick, S., Howsmon, J.A., Morehead, F.F. and Sisson, W.A., 1956. Level-off degree of polymerization. *Ind. Eng. Chem.* **48**: 333–335.

Bhattacharya, D., Germinario, L.T. and Winter, W.T., 2008. Isolation, preparation and characterization of cellulose microfibers obtained from bagasse. *Carbohydr. Polym.* **73**: 371–377.

Bledzki, A.K. and Gassan, J., 1999. Composites reinforced with cellulose based fibres. *Prog. Polym. Sci.* **24**: 221–274.

Bodycomb, J., Pejcinovic, M. and Hou, A., 2014. Introduction to Surface Area Analysis. HORIBA Scientific. www.horiba.com/us/particle. [Accessed on 15/12/2018 9:30 a.m].

Bolhuis, G.K., 1987. The effect on tablet crushing strength of magnesium stearate admixing in different types of lab-scale and production-scale mixers. *Pharm. Technol.* ***11***: 36-44.

BP (2009) British Pharmacopoeia Volume I & II Monographs: Medicinal and Pharmaceutical Substances Microcrystalline Cellulose.

Brebu, M. and Vasile, C., 2010. Thermal degradation of lignin-a review. *Cellul. Chem. Technol.* **44**: 353.

Burgina, E.B., Baltakhinov, V.P., Boldyreva, E.V. and Shakhtschneider, T.P., 2004. IR spectra of paracetamol and phenacetin. 1. Theoretical and experimental studies. *J. Struct. Chem.* ***45***: 64-73.

Calahorra, M.E., Cortazar, M., Eguiazabal, J.I. and Guzman, G.M., 1989. Thermogravimetric analysis of cellulose: effect of the molecular weight on thermal decomposition. *J. Appl. Polym. Sci.* **37**: 3305–3314.

Candido, R.G., and Gonçalves, A.R., 2016. Synthesis of cellulose acetate and carboxymethylcellulose from sugarcane straw. *Carbohydr. Polym.* **152**: 679–686.

Chufo, A., Yuan, H., Zou, D., Pang, Y. and Li, X., 2015. Biomethane production and physicochemical characterization of anaerobically digested Teff (*Eragrostis tef*) straw pretreated by sodium hydroxide. *Bioresour. Technol.* **181**: 214–219.

Cochrane, L. and Bekele, Y.W., 2018. Average crop yield (2001–2017) in Ethiopia: Trends at national, regional and zonal levels. *Data in brief*, *16*: 1025.

Coffey, D.G., Bell, D.A. and Henderson, A., 2006. Cellulose and cellulose derivatives. In: *Food polysaccharides and their applications*: 147–180.

Coleman, J.M., 2012. Assessing the Potential Use of Teff as an Alternative Grain Crop in Virginia (Doctoral dissertation, Virginia Tech): 3–5.

Cui, S.W., 2005. Polysaccharide Gums: Structures, Functional Properties, and Applications. In: *Food carbohydrates: chemistry, physical properties, and applications*. Taylor & Francis Group, LLC: 265–279.

Doelker, E., 1993. Comparative compaction properties of various microcrystalline cellulose types and generic products. *Drug Dev. Ind. Pharm.* **19**: 2399–2471.

Doelker, E., Gurny, R., Schurz, J., Janosi, A. and Matin, N., 1987. Degrees of crystallinity and polymerization of modified cellulose powders for direct tableting. *Powder Technol.* **52**: 207–213.

Doelker, E., Massuelle, D., Veuillez, F. and Humbert-Droz, P., 1995. Morphological, packing, flow and tableting properties of new Avicel types. *Drug Dev. Ind. Pharm.* **21**: 643–661.

Doesburg, J.J., 1957. Relation between the solubilization of pectin and the fate of organic acids during maturation of apples. *J. Sci. Food Agric.* **8**: 206–216.

Dourado, F., Gama, F.M., Chibowski, E. and Mota, M., 1998. Characterization of cellulose surface free energy. *J. Adhes. Sci. Technol.* **12**: 1081–1090.

Fan, M., Dai, D., and Huang, B., 2012. Fourier transform infrared spectroscopy for natural fibres. In: *Fourier transform-materials analysis*. InTech. 45–63.

Foodcomplex.org. http://foodcomex.org/foods/500. [Accessed: 12/9/18 10:57a.m].

Gerad, K. B. and Arne, W.H., 2011. Compaction properties of directly compressible materials. In: *Pharmaceutical powder compaction technology (2nd ed.)*. London: Informa Healthcare. 151–158.

Gerad, K.B and Hans, W., 2011. Lubrication issues in direct compaction. In: *Pharmaceutical powder compaction technology (2nd ed.)*. London: Informa Healthcare. 214–215.

Golbaghi, L., Khamforoush, M., & Hatami, T., 2017. Carboxymethyl cellulose production from sugarcane bagasse with steam explosion pulping: Experimental, modeling, and optimization. *Carbohydr. Polym.* **174**: 780–788.

Haafiz, M.M., Eichhorn, S.J., Hassan, A. and Jawaid, M., 2013. Isolation and characterization of microcrystalline cellulose from oil palm biomass residue. *Carbohydr. Polym.* **93**: 628–634.

Habib, Y., Augsburger, L., Reier, G., Wheatley, T. and Shangraw, R., 1996. Dilution potential: a new perspective. *Pharm. Dev. Tech.* **1**: 205–212.

Habibi, Y., Lucia, L.A. and Rojas, O.J., 2010. Cellulose nanocrystals: chemistry, self–assembly, and applications. *Chem. Rev.* **110**: 3479–3500.

Jahan, M.S., Rumee, J.N., Rahman, M.M. and Quaiyyum, A., 2014. Formic acid/acetic acid/water pulping of agricultural wastes. *Cellul. Chem. Technol.* **48**: 111–118.

Jahan, M.S., Saeed, A., He, Z. and Ni, Y., 2011. Jute as raw material for the preparation of microcrystalline cellulose. *Cellulose*, **18**:451–459.

Jiang, M., Zhao, M., Zhou, Z., Huang, T., Chen, X. and Wang, Y., 2011. Isolation of cellulose with ionic liquid from steam exploded rice straw. *Ind. Crop. Prod.* **33**: 734–738.

Jonoobi, M., Khazaeian, A., Tahir, P.M., Azry, S.S. and Oksman, K., 2011. Characteristics of cellulose nanofibers isolated from rubberwood and empty fruit bunches of oil palm using chemo-mechanical process. *Cellulose*, **18**: 1085–1095.

Karande, V.S., Bharimalla, A.K., Hadge, G.B., Mhaske, S.T. and Vigneshwaran, N., 2011. Nano-fibrillation of cotton fibers by disc refiner and its characterization. *Fibers Polym.* **12**: 399.

Karimi, K., and Taherzadeh, M.J., 2016. A critical review of analytical methods in pretreatment of lignocelluloses: composition, imaging, and crystallinity. *Bioresour. Technol.* **200**: 1008–1018.

Klemm, D., Heublein, B., Fink, H.P. and Bohn, A., 2005. Cellulose: fascinating biopolymer and sustainable raw material. *Angew. Chem. Int. Ed.* **44**: 3358–3393.

Klemm, D., Philpp, B., Heinze, T., Heinze, U. and Wagenknecht, W., 1998. Comprehensive cellulose chemistry. Volume 1: Fundamentals and analytical methods. Wiley-VCH Verlag GmbH.

Kornblum, S.S., and Stoopak, S.B., 1973. A New Tablet Disintegrant Agent: Cross-linked Polyvinylpyrrolidone. *J. Pharm. Sci.* **62**: 43–49.

Kothari, S.H., Kumar, V. and Banker, G.S., 2002. Comparative evaluations of powder and mechanical properties of low crystallinity celluloses, microcrystalline celluloses, and powdered celluloses. *Int. J. Pharm.* **232**: 69–80.

Kraemer, E.O., 1938. Molecular weights of celluloses and cellulose derivates. *Ind. Eng. Chem.* **30**: 1200–1203.

Kuentz, M. and Leuenberger, H., 2000. A new theoretical approach to tablet strength of a binary mixture consisting of a well and a poorly compactable substance. *Eur. J. Pharm. Biopharm.* **49**: 151–159.

Kumar, V., de la Luz Reus-Medina, M. and Yang, D., 2002. Preparation, characterization, and tableting properties of a new cellulose-based pharmaceutical aid. *Int. J. Pharm.* **235**: 129–140.

Lacasse, K. and Baumann, W., 2012. *Textile Chemicals: Environmental data and facts*. Springer Science & Business Media: 521–523.

Lachenal, D., and Chirat, C., 2005. Peracetic Acid Bleaching *Cellul. Chem. Technol.* **39**: 511–156.

Landin, M., Martinez-Pacheco R, Gomez-Amoza JL, Souto C, Concheiro, A. and Rowe, R.C., 1993a. "Effect of batch variation and source of pulp on the properties of microcrystalline cellulose." *Int. J. Pharm.* **91**: 133–141.

Landin, M., Martinez-Pacheco, R., Gomez-Amoza, J.L., Souto, C., Concheiro, A. and Rowe, R.C., 1993b. Effect of country of origin on the properties of microcrystalline cellulose. *Int. J. Pharm.* **91**: 123–131.

Lu, P., and Hsieh, Y.L., 2012. Preparation and characterization of cellulose nanocrystals from rice straw. *Carbohydr. Polym.* **87**: 564–573.

Malvern Instruments, 1999. Update for the MS2000 Operators guide. Worcestershire, United Kingdom: Malvern Instruments.

Marchessault, R.H., 1962. Application of infra-red spectroscopy to cellulose and wood polysaccharides. *Pure Appl. Chem.* **5**: 107–130.

Mengesha, M.H., 1966. Chemical composition of Teff (*Eragrostis tef*) compared with that of wheat, barley and grain sorghum. *Econ. Bot.* **20**: 268–273.

Miller, D.L., 1975. Annual crops-a renewable source for cellulose. *J. Appl. Polymer Sci.* **28: 21**–**28**.

Mire, M.A., Benjelloun-Mlayah, B., Delmas, M. and Bravo, R., 2005. Formic acid/acetic acid pulping of banana stem (Musa Cavendish). *Appita Journal: J. Tech. Assoc. Aust. New Zealand Pulp Pap. Ind.* **58:** p.393.

Montané, D., Farriol, X., Salvadó, J., Jollez, P. and Chornet, E., 1998. Fractionation of wheat straw by steam-explosion pretreatment and alkali delignification. Cellulose pulp and byproducts from hemicellulose and lignin. *J. Wood Chem. Technol.* **18**: 171–191.

Moreira, L.M., Leonel, F.D.P., Vieira, R.A.M. and Pereira, J.C., 2013. A new approach about the digestion of fibers by ruminants. *Rev. Bras. Saúde Prod. Anim.* **14**: 382–395.

Mottaleb, K.A. and Rahut, D.B., 2018. Household production and consumption patterns of Teff in Ethiopia. *Agribusiness* **34**: 668–684.

Nelson, M.L. and O'Connor, R.T., 1964. Relation of certain infrared bands to cellulose crystallinity and crystal lattice type. Part II. A new infrared ratio for estimation of crystallinity in celluloses I and II. *J. Appl. Polym. Sci.* **8**: 1325–1341.

Nokhodchi, A., 2005. Effect of moisture on compaction and compression. *Pharm. Tech.* **6***:* 46–66.

Nuruddin, M., Chowdhury, A., Haque, S.A., Rahman, M., Farhad, S.F., Jahan, M.S. and Quaiyyum, A., 2011. Extraction and characterization of cellulose microfibrils from

agricultural wastes in an integrated biorefinery initiative. *Cellul. Chem. Technol.* **45**: 347–354.

Obae, K., Iijima, H. and Imada, K., 1999. Morphological effect of microcrystalline cellulose particles on tablet tensile strength. *Int. J. Pharm.* **182**: 155–164.

Padmadisastra, Y. and Gonda, I., 1989. Preliminary studies of the development of a direct compression cellulose excipient from bagasse. *J. Pharm. Sci*. **78**:508–514.

Painer, D., Lux, S. and Siebenhofer, M., 2015. Recovery of formic acid and acetic acid from waste water using reactive distillation. *Sep. Sci. Technol.* **50**: 2930–2936.

Park, S., Johnson, D.K., Ishizawa, C.I., Parilla, P.A. and Davis, M.F., 2009. Measuring the crystallinity index of cellulose by solid state 13C nuclear magnetic resonance. *Cellulose* **16**: 641–647.

Peng, Y., Han, Y. and Gardner, D.J., 2012. Spray-drying cellulose nanofibrils: effect of drying process parameters on particle morphology and size distribution. *Wood Fiber Sci.* **44**: 448-461.

Pesonen, T. and Paronen, P., 1986. Evaluation of a new cellulose material as binding agent for direct compression of tablets. *Drug Dev. Ind. Pharm.* **12**: 2091–2111.

Pesonen, T., Paronen, P. and Puurunen, T., 1989. Evaluation of a novel cellulose powder as a filler-binder for direct compression of tablets. *Pharm. Weekbl. (Sci)* **11**: 13–19.

Radotić, K. and Mićić, M., 2016. Methods for Extraction and Purification of Lignin and Cellulose from Plant Tissues. In: *Sample Preparation Techniques for Soil, Plant, and Animal Samples*. Humana Press, New York, NY: 365–376.

Ramiah, M.V., 1970. Thermogravimetric and differential thermal analysis of cellulose, hemicellulose, and lignin. *J. Appl. Polym. Sci.* **14**: 1323–1337.

Rojas, J. and Kumar, V., 2012. Evaluation of the disintegration properties of microcrystalline cellulose II and commercial disintegrants. *Pharmazie **67***: 500-506.

Roseberg, R.J., Norberg, S., Smith, J., Charlton, B., Rykbost, K. and Shock, C., 2006. Yield and quality of teff forage as a function of varying rates of applied irrigation and

nitrogen. *Research in the Klamath Basin 2005 Annual Report. OSU-AES Special Report*, **1069**: 119–136.

Rowe, R.C., Sheskey, P.J. and Owen, S.C. eds., 2009. Handbook of pharmaceutical excipients (6th ed). London: Pharmaceutical press: 129–133.

Saxena, I., and Brown, M., 2005. Cellulose Biosynthesis: Current Views and Evolving Concepts. *Ann. Bot.* **96**: 9–21.

Segal, L.G.J.M.A., Creely, J.J., Martin Jr, A.E. and Conrad, C.M., 1959. An empirical method for estimating the degree of crystallinity of native cellulose using the X-ray diffractometer. *Text. Res. J.*, **29**: 786–794.

Silverstein, R.M., Webster, F.X., Kiemle, D.J. and Bryce, D.L., 2011. Infrared Spectroscopy. In: *Spectrometric identification of organic compounds (7th ed)*. John Wiley & Sons, Ltd: 72–126.

Spiridon, I., 2018. Biological and Pharmaceutical Applications of Lignin and its Derivatives: A Mini-Review. *Cellul. Chem. Technol.* **52**: 543–550.

Stallknecht, G.F., K.M. Gilbertson, and J.L. Eckhoff. 1993. Teff: Food crop for humans and animals. In: *J. Janick and J.E. Simon (eds.), New crops.* Wiley, New York: 231–234.

Stuart, B., 2004. Organic molecules. In: *Infrared spectroscopy: Fundamental and applications.* John Wiley & Sons, Ltd: 71–93.

Sun J.X., Sun, X.F., Zhao, H., Sun, R.C., 2004. Isolation and characterization of cellulose from sugarcane bagasse. *Polym. Degrad. Stab.* **84**: 331–339.

Sun, C.C., 2008. Mechanism of moisture induced variations in true density and compaction properties of microcrystalline cellulose. *Int. J. Pharm.* **346**: 93–101.

Sun, R. and Hughes, S., 1998. Fractional extraction and physico-chemical characterization of hemicelluloses and cellulose from sugar beet pulp. *Carbohydr. Polym.* **36**: 293–299.

Sun, S., Sun, S., Cao, X. and Sun, R., 2016. The role of pretreatment in improving the enzymatic hydrolysis of lignocellulosic materials. *Bioresour. Technol.* **199**: 49–58.

Sun, X.F., Xu, F., Sun, R.C., Fowler, P. and Baird, M.S., 2005. Characteristics of degraded cellulose obtained from steam-exploded wheat straw. *Carbohydr. Res.* **340**: 97–106.

Suzuki, T. and Nakagami, H., 1999. Effect of crystallinity of microcrystalline cellulose on the compactibility and dissolution of tablets. *Eur. J. Pharm. Biopharm.* **47**: 225–230.

Terinte, N., Ibbett, R. and Schuster, K.C., 2011. Overview on native cellulose and microcrystalline cellulose I structure studied by X-ray diffraction (WAXD): Comparison between measurement techniques. *Lenzinger Berichte*, **89**: 118–131.

Thoorens, G., Krier, F., Leclercq, B., Carlin, B. and Evrard, B., 2014. Microcrystalline cellulose, a direct compression binder in a quality by design environment–A review. *Int. J. Pharm*. **473**: 64–72.

Trache, D., Donnot, A., Khimeche, K., Benelmir, R. and Brosse, N., 2014. Physico-chemical properties and thermal stability of microcrystalline cellulose isolated from Alfa fibres. *Carbohydr. Polym.* **104**: 223–230.

Trache, D., Hussin, M. H., Chuin, C. T. H., Sabar, S., Fazita, M. N., Taiwo, O. F., Hassan, T.M. & Haafiz, M. M. (2016). Microcrystalline cellulose: Isolation, characterization and bio–composites application-A review. *Int. J. Biol. Macromol.* **93**: 789–804.

USP30 - NF25, 2007. United States Pharmacopeia and National Formulary. Rockville, MD: United States Pharmacopeial Convention.

USP30 - NF25: Chapter 1174, 2007. Powder flow. In: *United States Pharmacopeia and National Formulary (USP30 - NF25).* Rockville, MD: United States Pharmacopeial Convention.

USP30 - NF25: Chapter 616, 2007. Bulk density and tapped density. In: *United States Pharmacopeia and National Formulary (USP30 - NF25).* Rockville, MD: United States Pharmacopeial Convention.

USP30 - NF25: Chapter 701, 2007. Disintegration. In: *United States Pharmacopeia and National Formulary (USP30 - NF25).* Rockville, MD: United States Pharmacopeial Convention.

Van Heiningen, A., 2006. Converting a Kraft pulp mill into an integrated forest biorefinery. *Pulp Pap. Canada* **107**: 38–43.

Vanderghem, C., Brostaux, Y., Jacquet, N., Blecker, C. and Paquot, M., 2012. Optimization of formic/acetic acid delignification of Miscanthus x giganteus for enzymatic hydrolysis using response surface methodology. *Ind. Crop Prod.* **35**: 280–286.

Varshney, V.K. and Naithani, S., 2011. Chemical functionalization of cellulose derived from nonconventional sources. In: *Cellulose Fibers: Bio-and Nano-Polymer Composites*. Springer, Berlin, Heidelberg: 43–60.

Vromans, H., Bolhuis, G.K. and Lerk, C.F., 1988. Magnesium stearate susceptibility of directly compressible materials as an indication of fragmentation properties. *Powder Technol.* **54**: 39–44.

Wang, D., Shang, S.B., Song, Z.Q. and Lee, M.K., 2010. Evaluation of microcrystalline cellulose prepared from kenaf fibers. *J. Ind. Eng. Chem.* **16**: 152–156.

Wassie, A.B. and Srivastava, V.C., 2016. Teff straw characterization and utilization for chromium removal from wastewater: kinetics, isotherm and thermodynamic modelling. *J Env. Chem. Eng.* **4**: 1117–1125.

Williams, R.O., Sriwongjanya, M. and Barron, M.K., 1997. Compaction properties of microcrystalline cellulose using tableting indices. *Drug Dev. Ind. Pharm.* **23**: 695–704.

Yang, H., Yan, R., Chen, H., Lee, D.H. and Zheng, C., 2007. Characteristics of hemicellulose, cellulose and lignin pyrolysis. *Fuel* **86**: 1781–1788.

Zaki, H.M., 2011. Spectroscopy surface analysis of paracetamol and paracetamol and excipient systems (Doctoral dissertation, The University of Manchester (United Kingdom)).

Zhang, M., Qi, W., Liu, R., Su, R., Wu, S., He, Z., 2010. Fractionating lignocellulose by formic acid: Characterization of major components. *Biomass Bioenergy* **34**: 525–532.